The Chlamydomonas deg1c Mutant Accumulates Proteins Involved in High Light Acclimation

Jasmine Theis, Julia Lang, Benjamin Spaniol, Suzanne Ferté, Justus Niemeyer, Frederik Sommer, David Zimmer, Benedikt Venn, Shima Farazandeh Mehr, Timo Mühlhaus, et al.

The *Chlamydomonas deg1c* Mutant Accumulates Proteins Involved in High Light Acclimation[1][OPEN]

Jasmine Theis,[a] Julia Lang,[a] Benjamin Spaniol,[a] Suzanne Ferté,[b] Justus Niemeyer,[a] Frederik Sommer,[a] David Zimmer,[a] Benedikt Venn,[a] Shima Farazandeh Mehr,[a] Timo Mühlhaus,[a] Francis-André Wollman,[b] and Michael Schroda[a,2,3]

[a]Molekulare Biotechnologie & Systembiologie, Technische Universität Kaiserslautern, Paul-Ehrlich D-67663 Kaiserslautern, Germany
[b]Laboratoire de Physiologie Membranaire et Moléculaire du Chloroplaste, Institut de Biologie Physico-Chimique, UMR CNRS/UPMC 7141, Paris, France

ORCID IDs: 0000-0002-8680-4688 (J.L.); 0000-0001-8738-9554 (B.S.); 0000-0003-4203-1596 (B.V.); 0000-0003-3925-6778 (T.M.); 0000-0003-2638-7840 (F.-A.W.); 0000-0001-6872-0483 (M.S.).

Degradation of periplasmic proteins (Deg)/high temperature requirement A (HtrA) proteases are ATP-independent Ser endopeptidases that perform key aspects of protein quality control in all domains of life. Here, we characterized *Chlamydomonas reinhardtii* DEG1C, which together with DEG1A and DEG1B is orthologous to Arabidopsis (*Arabidopsis thaliana*) Deg1 in the thylakoid lumen. We show that DEG1C is localized to the stroma and the periphery of thylakoid membranes. Purified DEG1C exhibited high proteolytic activity against unfolded model substrates and its activity increased with temperature and pH. DEG1C forms monomers, trimers, and hexamers that are in dynamic equilibrium. DEG1C protein levels increased upon nitrogen, sulfur, and phosphorus starvation; under heat, oxidative, and high light stress; and when Sec-mediated protein translocation was impaired. DEG1C depletion was not associated with any obvious aberrant phenotypes under nonstress conditions, high light exposure, or heat stress. However, quantitative shotgun proteomics revealed differences in the abundance of 307 proteins between a *deg1c* knock-out mutant and the wild type under nonstress conditions. Among the 115 upregulated proteins are PSII biogenesis factors, FtsH proteases, and proteins normally involved in high light responses, including the carbon dioxide concentrating mechanism, photorespiration, antioxidant defense, and photoprotection. We propose that the lack of DEG1C activity leads to a physiological state of the cells resembling that induced by high light intensities and therefore triggers high light protection responses.

Members of the high temperature requirement A (HtrA) family of ATP-independent Ser endopeptidases are found in all domains of life, including Archaea, Bacteria, and Eukarya (Pallen and Wren, 1997; Clausen et al., 2011; Hansen and Hilgenfeld, 2013). They perform key aspects of protein quality control due to their ability to rapidly sense misfolded proteins and degrade them following the inducible activation of proteolytic activity. The first HtrA family member, DegP, was identified in *Escherichia coli* as a protein required for cell viability at high temperatures (Lipinska et al., 1989) and responsible for the degradation of abnormal periplasmic proteins (Strauch and Beckwith, 1988). DegP cleaves solvent-exposed peptide bonds of Val-X or Ile-X, a typical feature of unfolded proteins exposing their hydrophobic core (Kolmar et al., 1996).

In addition to their proteolytic activity, HtrA family members have been reported to possess chaperone activity that, for example, allows them to promote refolding of the unfolded MalS protein (Spiess et al., 1999) and assembly of PSII dimers and supercomplexes (Sun et al., 2010b), or to stabilize folding intermediates of outer membrane proteins (Krojer et al., 2008). However, this chaperone activity has been challenged recently (Ge et al., 2014; Chang, 2016).

HtrA family members contain an N-terminal protease domain with the His-Asp-Ser catalytic triad and usually at least one C-terminal PDZ domain (Clausen et al., 2002). All HtrA family members form homotrimers that are stabilized by extensive contacts between the

[1]This work was supported by the Deutsche Forschungsgemeinschaft (SFB/TRR175 and FOR2092 to M.S.) and the European Research Council (Photophytomics starting grant to S.F.).

[2]Author for contact: schroda@bio.uni-kl.de.
[3]Senior author.

The author responsible for distribution of materials integral to the findings presented in this article in accordance with the policy described in the Instructions for Authors (www.plantphysiol.org) is: Michael Schroda (schroda@bio.uni-kl.de).

J.T. performed most of the experiments. J.L. and B.S. performed the protease activity assays and verified the proteomics results on *DEG1C*-amiRNA lines and the lack of phenotypes in the *deg1c* mutant. S.F. performed the electrochromic shift measurements, supervised by F.-A.W. J.N. performed the acetate consumption experiments. F.S. ran the mass spectrometry analyses. D.Z. did the data analysis, supervised by T.M. B.V. genotyped the *deg1c* knock-out mutant. M.S. supervised the work and wrote the article with contributions from the other authors.

[OPEN]Articles can be viewed without a subscription.
www.plantphysiol.org/cgi/doi/10.1104/pp.19.01052

three protease domains (Krojer et al., 2002, 2008; Kley et al., 2011). In the absence of substrates, HtrA trimers are inactive, because loops composing the active site are disordered. Their disorder-order transition, leading to the establishment of the active site, requires the interaction of loops between neighboring protomers, which is eventually triggered by substrate binding (Hasselblatt et al., 2007; Krojer et al., 2010; Merdanovic et al., 2010; Truebestein et al., 2011).

Arabidopsis (*Arabidopsis thaliana*) encodes 16 HtrA family members (Deg1–Deg16), of which at least five localize to chloroplasts (Schuhmann et al., 2012). There, Deg2 and Deg7 are associated with the stromal side of thylakoid membranes (Haussühl et al., 2001; Sun et al., 2010a), while Deg1, Deg5, and Deg8 are associated with the lumenal side (Itzhaki et al., 1998; Sun et al., 2007). Deg5 lacks a PDZ domain and forms heterooligomeric complexes with Deg8 in a 1:1 stoichiometry (Sun et al., 2007; Butenko et al., 2018). The proteolytic activity of Deg1 and Deg2 was shown to depend on the redox state, with Deg1 being more active under reducing conditions and Deg2 more active under oxidizing conditions (Ströher and Dietz, 2008). Furthermore, Deg1 undergoes a pH-dependent switch from the inactive monomer (at pH 8.0) to the proteolytically active, hexameric state (at pH 6.0) through protonation of His-244 (Chassin et al., 2002; Kley et al., 2011). Acidification of the thylakoid lumen occurs during high light exposure, when also the rate of damage to photosynthetic proteins increases. The D1 subunit of PSII is most prone to photodamage, requiring continuous degradation and replacement by a newly synthesized copy (Theis and Schroda, 2016). Consistently, Deg1, Deg5, Deg7, and Deg8 have been found to participate in PSII repair by cleaving photodamaged D1 within different loops connecting the transmembrane helices (Kapri-Pardes et al., 2007; Sun et al., 2007, 2010a; Knopf and Adam, 2018). Moreover, recombinant Deg1 has been shown to degrade plastocyanin and OE33 in vitro (Chassin et al., 2002), as well as D2, CP26 (Lhcb5), CP29 (Lhcb4), cytochrome b_6, and PsbS in high light-treated thylakoid membranes (Zienkiewicz et al., 2012). Deg2 has been shown to degrade light-harvesting protein Lhcb6 following high-salt, wounding, high-temperature, and high-irradiance stress (Luciński et al., 2011).

With 15 genes encoding HtrA family members in *Chlamydomonas reinhardtii,* the number of HtrA protein-encoding genes appears to be comparable between Arabidopsis and *Chlamydomonas*. However, as pointed out by Schuhmann et al. (2012), the "core set" of conserved HtrA protease types, found in every plant organism with at least one copy, consists of only eight members. This conserved core set consists of Deg1, Deg5, and Deg8 in the thylakoid lumen, Deg2 and Deg7 in the chloroplast stroma, Deg9 in the nucleolus, Deg15 in the peroxisome, and Deg10 in mitochondria. Here, it is interesting that organism-specific expansions of *HtrA* gene copy numbers in different branches of the phylogenetic tree have taken place. An example of such an organism-specific multiplication of an HtrA core set member is Deg1: only one form of the protein exists in Arabidopsis, rice (*Oryza sativa*), poplar (*Populus* spp.), and *Physcomitrella patens*, while there are three Deg1 forms in *Chlamydomonas*, termed DEG1.1, DEG1.2, and DEG1.3 (Schuhmann et al., 2012). In line with *Chlamydomonas* gene nomenclature, these proteins were termed DEG1A, DEG1B, and DEG1C, respectively, and, based on their strong similarity with Arabidopsis Deg1, are proposed to localize to the thylakoid lumen (Schroda and Vallon, 2009). In contrast, both *Chlamydomonas* and Arabidopsis encode only single members of lumenal Deg5 and Deg8 and of stromal Deg2 and Deg7 (Schuhmann et al., 2012).

Here, we have characterized the *Chlamydomonas* DEG1C protease. DEG1C raised our interest because its expression levels were found to increase in response to various stress conditions, such as treatment with the photosensitizer neutral red, sulfur and phosphorus starvation, long-term heat stress, and depletion of the chloroplast ClpP protease (Zhang et al., 2004; Fischer et al., 2005; Moseley et al., 2006; Ramundo et al., 2014; Schroda et al., 2015).

RESULTS

Proteolytic Activity of DEG1C Depends on the Folding State of the Substrate, pH, and Temperature

To investigate the enzymatic properties of DEG1C, we recombinantly expressed the protein without its chloroplast transit peptide in *E. coli* and purified the protein by chitin-affinity chromatography. We analyzed its activity on several model substrates that have been used previously for protease activity assays with HtrA proteins, i.e. casein, malate dehydrogenase (MDH), lysozyme, and bovine serum albumin (BSA; Lipinska et al., 1990; Kolmar et al., 1996; Kim et al., 1999; Chassin et al., 2002; Murwantoko et al., 2004; Sun et al., 2007; Krojer et al., 2008; Jomaa et al., 2009; Shen et al., 2009; Knopf and Adam, 2018). We first incubated recombinant DEG1C with a mixture of casein α-, β-, and κ-chains and MDH at 40°C with a 10-fold molar excess of substrate. All casein proteins had already been proteolytically attacked after 5 min of incubation, and the maximum extent of degradation was reached after 30 min (Fig. 1A). MDH was completely degraded within 2 h (Fig. 1B). To test whether proteolytic activity depends on the folding state of the substrate, we incubated the globular proteins lysozyme and BSA with DEG1C for 2 h at 40°C in the presence of dithiothreitol (DTT) to induce protein unfolding (Murwantoko et al., 2004). As shown in Figure 1, C and D, lysozyme and BSA were degraded by DEG1C if DTT was present in the reaction. In the absence of DTT, BSA was not degraded, pointing to the preference of DEG1C for unfolded substrates. Neither of the tested substrates was degraded in the absence of DEG1C, thus excluding degradation by contaminating proteases. The degradation of lysozyme was strongly reduced in the presence of the Ser protease inhibitor phenylmethylsulfonyl fluoride (Supplemental Fig. S1A).

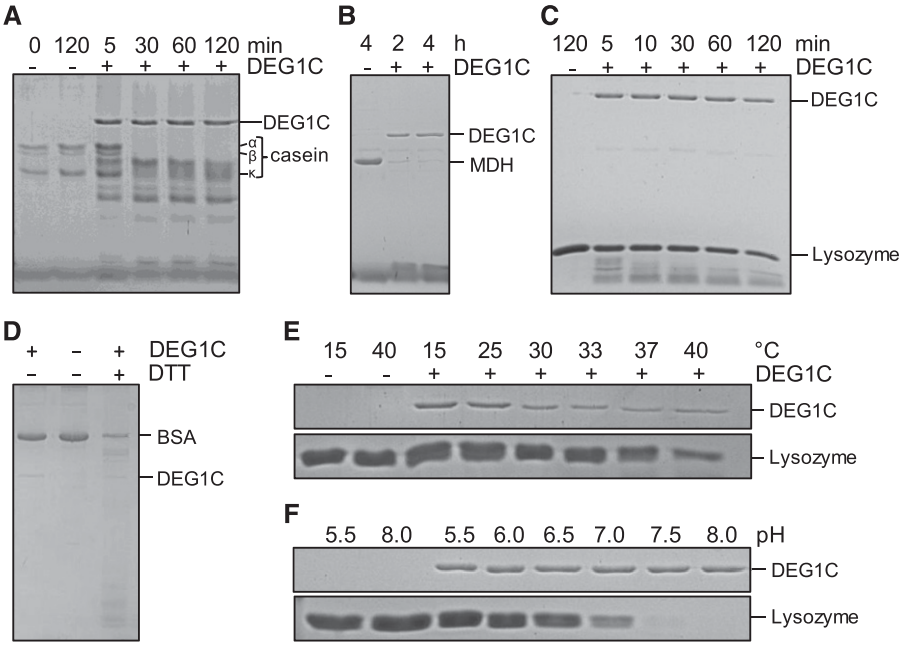

Figure 1. The proteolytic activity of DEG1C against model substrates depends on the folding state, pH value, and incubation temperature of the substrates. A, Purified DEG1C was incubated with a mixture of α-, β-, and κ-forms of naturally unfolded casein at 40°C and pH 7.4 for 2 h. B, Purified DEG1C was incubated with MDH at 40°C and pH 7.4 for 4 h. C, Purified DEG1C was incubated with lysozyme at 40°C and pH 7.4 for 2 h. The reaction contained 2 mM DTT to induce lysozyme unfolding. D, Purified DEG1C was incubated with BSA at 40°C and pH 7.4 for 2 h. Where indicated, the reaction contained 2 mM DTT to induce the unfolding of BSA. E, Purified DEG1C was incubated with lysozyme at the indicated temperatures and pH 7.4 for 2 h in the presence of 2 mM DTT. F, Purified DEG1C was incubated with lysozyme at 40°C and the indicated pH values for 2 h in the presence of 2 mM DTT. In all assays, concentrations of DEG1C and model substrates were 1.3 μM and 13 μM, respectively. Samples were separated on 12% SDS-polyacrylamide gels and stained with Coomassie blue.

Using DTT-unfolded lysozyme, we next tested whether the proteolytic activity of DEG1C increased with increasing temperatures. Below 37°C, DEG1C proteolytic activity was low, but it increased when the temperature was elevated to 37°C and above (Fig. 1E). To also test whether the proteolytic activity of DEG1C was pH dependent, we incubated DEG1C with DTT-unfolded lysozyme at pH values ranging from 5.5 to 8.0. While proteolytic activity was low at pH 5.5, it increased with rising pH and was maximal at pH 7.5 and 8.0 (Fig. 1F). The same dependence of DEG1C on temperature and pH was observed with naturally unfolded casein as substrate (Supplemental Figs. S1B and S1C). In our assays, we routinely observed a reduction in the amount of DEG1C protein during incubation, pointing to some autoproteolytic activity of the protease, which has been observed for other HtrA members as well (Kim et al., 1999; Chassin et al., 2002; Krojer et al., 2008; Jomaa et al., 2009).

DEG1C Is an Abundant Protein Localized in the Chloroplast Stroma and to the Stromal Side of Thylakoid Membranes

We raised a polyclonal antiserum against the DEG1C protein and detected the protease in *Chlamydomonas* whole-cell extracts by immunoblotting using affinity-purified antibodies. These procedures detected two protein bands with apparent masses of 51.2 and 45.5 kD (Fig. 2A). To identify the proteins in the two bands, we immunoprecipitated DEG1C from soluble *Chlamydomonas* proteins with the affinity-purified antibodies. Immunoprecipitated proteins were separated on an SDS gel and the excised protein bands were subjected to tryptic in-gel digestion and analysis by liquid chromatography-tandem mass spectrometry (LC-MS/MS). We found 36 peptides for DEG1C and two for DEG1B (Supplemental Fig. S2). Thus, the 45.5- and 51.2-kD proteins can be assigned to DEG1C and DEG1B, respectively.

The tryptic peptides covered 64% of the DEG1C amino acid sequence. While the first 132 amino acids were not covered at all, the remaining protein was homogeneously covered (Supplemental Fig. S2), suggesting that the noncovered 132 amino acids represent the chloroplast transit peptide. Hence, the mature DEG1C protein has a calculated molecular mass of 40.2 kD and migrates with an apparent mass ~12% larger than the calculated molecular mass in SDS-PAGE.

To get an estimate of its cellular abundance, we detected DEG1C immunologically in dilution series of whole-cell proteins and recombinant DEG1C (Fig. 2B). Quantification of three independent experiments revealed that DEG1C represents 0.012% ± 0.003% of total cellular

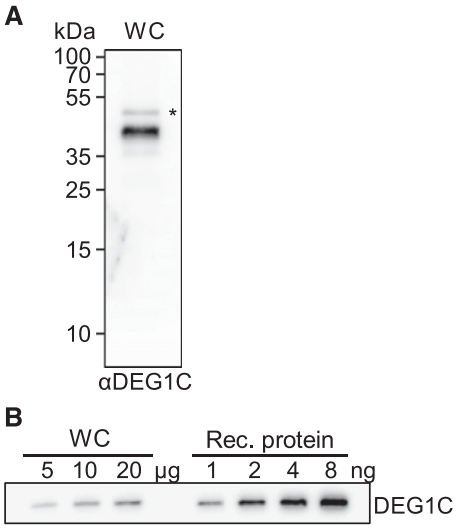

Figure 2. Characterization of the DEG1C antiserum and quantification of the cellular abundance of DEG1C. A, Immunodetection of DEG1C in cw15-325 whole-cell proteins (WC) corresponding to 2 μg chlorophyll. The asterisk marks DEG1B cross-reacting with affinity-purified DEG1C antibodies. B, The indicated amounts of *Chlamydomonas* whole-cell proteins (μg) and recombinant (rec.) DEG1C (ng) were separated on a 12% SDS polyacrylamide gel and analyzed by immunoblotting.

proteins. *Chlamydomonas* cells have a volume of ~270 μm^3 and contain ~20 pg protein (Weiss et al., 2000; Hammel et al., 2018), leading to a cellular protein concentration of ~74 mg/mL. With DEG1C localizing to the chloroplast, which makes up about half the volume of a *Chlamydomonas* cell (Weiss et al., 2000), the in vivo concentration of DEG1C is about 0.018 mg/mL, or 0.45 μM.

Based on its N-terminal extension and the localization of the Arabidopsis ortholog Deg1, *Chlamydomonas* DEG1C was proposed to be targeted to the thylakoid lumen (Schroda and Vallon, 2009). To verify this localization, we fractionated *Chlamydomonas* whole cells into chloroplasts, stroma, thylakoids, and mitochondria. The purity of the fractions was tested by immunoblot analyses using antibodies against mitochondrial carbonic anhydrase, stromal CGE1 (chloroplast GrpE homolog 1), and the integral thylakoid membrane protein cytochrome *f* (Fig. 3A). As judged from the signals obtained with these control antibodies, mitochondria were largely free of chloroplast proteins. The chloroplast stroma and thylakoid fractions were not cross-contaminated. However, thylakoids were contaminated with mitochondria. DEG1C was detected in the chloroplast preparation and in the stroma and thylakoid membrane fractions. When compared with stromal CGE1, much more DEG1C was detected in the thylakoid membrane fraction, indicating that part of DEG1C is associated with thylakoid membranes. The chloroplast localization of *DEG1C* was confirmed by immunofluorescence microscopy, with chloroplast HSP90C serving as control (Fig. 3B).

Next, we analyzed the nature of the interaction of DEG1C with thylakoid membranes. For this, cells were lysed by three freezing and thawing cycles, in the presence of either a low-salt buffer, or the same buffer supplemented with 200 mM Na_2CO_3. Lysis in the presence of Na_2CO_3 resulted in an almost complete release of DEG1C from the membranes (Fig. 3C). Likewise, the β-subunit of chloroplast ATP synthase (CF1β), as well as PSI subunit N (PSAN), both peripherally attached to the stromal and lumenal sides, respectively, of thylakoid membranes, were recovered in the soluble fraction. In contrast, the integral membrane protein cytochrome *f* was not released from the membranes by the salt treatment. These data indicate that DEG1C is peripherally associated with thylakoid membranes. To address whether DEG1C is associated with the stromal or the lumenal side, isolated thylakoids were incubated with trypsin. As shown in Figure 3D, DEG1C was degraded by trypsin like HSP70B, which for the most part is localized in the

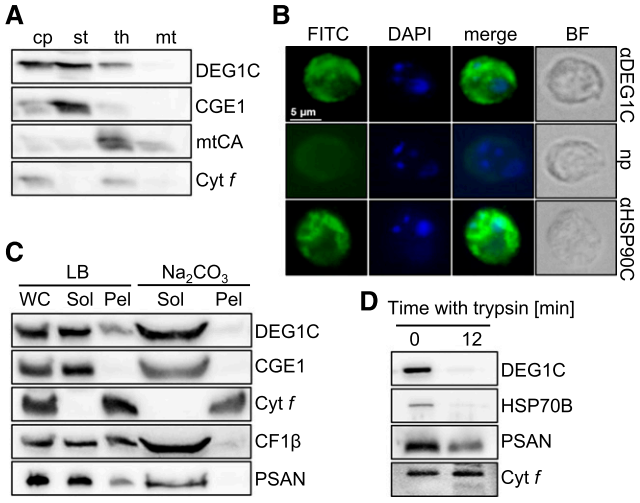

Figure 3. Subcellular localization of DEG1C. A, Mitochondria (mt) and chloroplasts (cp) were isolated from *Chlamydomonas* strain CF185. Chloroplasts were further fractionated into stroma (st) and thylakoid membranes (th). From each fraction, 5 μg of protein was separated on a 12% SDS-polyacrylamide gel and analyzed by immunoblotting using antisera against DEG1C, stromal CGE1, mitochondrial carbonic anhydrase (mtCA), and integral thylakoid membrane protein cytochrome *f* (Cyt *f*). B, cw15-325 cells grown at ~30 μmol photons m^{-2} s^{-1} were analyzed by immunofluorescence microscopy. Shown from left to right are immunofluorescence images of cells decorated with a fluorescein isothiocyanate (FITC)-labeled secondary antibody, stained with DAPI, a merge of the DAPI and FITC images, and bright-field (BF) images. Cells were incubated with primary antibodies against DEG1C and HSP90C, and withoutprimary antibody (np). C, cw15-325 whole cells (WC) were resuspended in lysis buffer (LB) alone (10 mM Tris-HCl, pH 8, 1 mM EDTA, protease inhibitor cocktail) or LB containing 200 mM Na_2CO_3, subjected to three cycles of freezing and thawing, and centrifuged to separate soluble (Sol) and pellet (Pel) fractions. Proteins were separated on a 12% SDS polyacrylamide gel and analyzed by immunoblotting. D, Isolated thylakoids from strain cw15-325 were incubated on ice with 0.0625 mg mL^{-1} trypsin. Thylakoid membrane proteins were then separated on a 12% SDS-polyacrylamide gel and analyzed by immunoblotting.

stroma and is associated to a lesser extent with membranes (Schroda et al., 2001). In contrast, lumenal PSAN was much more protected from the protease treatment, and trypsin had no effect on the intrinsic membrane protein cytochrome *f*. These results indicate that, like HSP70B, *Chlamydomonas* DEG1C is largely localized to the chloroplast stroma, with a smaller fraction of the protein being associated with thylakoid membranes.

DEG1C Accumulates under Various Stress Conditions

DegP is indispensable for the survival of *E. coli* at elevated temperatures (Lipinska et al., 1989), and DegP protein levels increased under oxidative and reducing conditions as well as under heat stress (Skórko-Glonek et al., 2003). Moreover, Arabidopsis Deg1 protein and transcript levels were found to increase under heat and high light stress, respectively (Itzhaki et al., 1998; Sinvany-Villalobo et al., 2004). We therefore tested the expression of DEG1C under heat, high light, and H_2O_2 stress. As shown in Figure 4, A and G, we found that *Chlamydomonas* DEG1C protein levels increased on average by 4.7-fold after 6 h of heat stress. Exposure to high light and H_2O_2 for 6 h led to milder increases in DEG1C levels by 2.4- and 1.7-fold, respectively (Figs. 4, B, C, and G).

Microarray analyses revealed that *DEG1C* gene expression is modestly increased during sulfur and phosphate starvation (Zhang et al., 2004; Moseley et al., 2006). To analyze changes in DEG1C protein abundance in response to nutrient limitation, we monitored DEG1C protein levels during nitrogen, phosphate, and sulfur deprivation. As shown in Figure 4, D–F and G, levels of DEG1C increased dramatically, on average by 10- and 11-fold after 48 h of P- and N-starvation, respectively, and by 17.5-fold after 52 h of S-starvation.

So far, our data indicate a role of DEG1C in the quality control and/or remodeling of chloroplast proteins under acute stress and nutrient limitation. To test more specifically for a role in protein quality control, we monitored DEG1C accumulation in strains harboring a nitrate-inducible artificial microRNA (amiRNA) construct targeting the *SECA* transcript. SECA is an essential component of the thylakoidal Sec pathway. As shown in Figure 4H, DEG1C levels increased when the amiRNA against *SECA* was induced by growing cells on nitrate-containing medium. However, although the SECA protein was no longer detectable after only 18 h of growth on this medium, DEG1C accumulated only between 24 h and 42 h of growth on nitrate-containing medium. Growth on nitrate itself did not induce the accumulation of DEG1C.

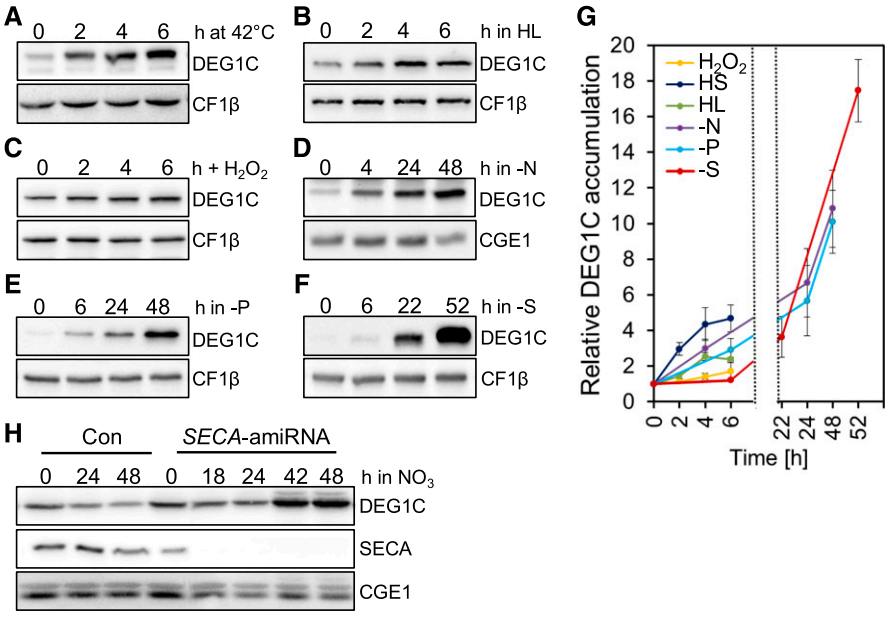

Figure 4. Analysis of conditions leading to an increased abundance of DEG1C. A, Exposure of CC-124 cells to 42°C for 6 h. B, Exposure of CC-124 cells to high light (HL) intensities of 800 μmol photons m^{-2} s^{-1} for 6 h. C, Incubation of CC-124 cells with 2 mM H_2O_2 for 6 h. D, CC-124 cells were harvested, washed, resuspended in TAP-N, and cultivated for 48 h in TAP-N. E, CC-124 cells were harvested, washed, resuspended in TAP-P, and cultivated for 48 h in TAP-P. F, CC-124 cells were harvested, washed, resuspended in TAP-S, and cultivated for 52 h in TAP-S. G, Quantification of DEG1C protein abundance from three independent experiments for each of the conditions shown in A–F using the FUSIONCapt Advance program. Signals were normalized to the initial DEG1C levels. Error bars represent the SD. H, cw15-325 cells were transformed with an empty amiRNA vector driven by the nitrate reductase promoter (Con) or the same vector containing a small interfering RNA against *SECA*. Cells were harvested, washed, resuspended in TAP medium containing nitrate (NO_3), and cultivated for 48 h in TAP-NO_3. If not indicated otherwise, cells were grown in TAP medium at a light intensity of 30 μmol photons m^{-2} s^{-1}.

Depletion of DEG1C Has No Obvious Phenotypes on *Chlamydomonas* under Control, High Light, and Heat Stress Conditions

To get insights into the in vivo function of DEG1C, we transformed *Chlamydomonas* cells with a vector for the constitutive expression of an amiRNA targeting *DEG1C* (Molnár et al., 2007; Supplemental Fig. S3A). With this approach, we were routinely able to generate transformants with DEG1C protein levels reduced to ~10% of wild-type levels (Supplemental Fig. S3B). However, under standard growth conditions we observed no significant differences between control and *DEG1C*-amiRNA lines regarding cell morphology, chlorophyll content per cell, chlorophyll *a*/*b* ratio, generation time, or cell diameter (Supplemental Fig. S4).

Members of the chloroplast Deg family in Arabidopsis—Deg1, Deg5, Deg7, and Deg8—cleave photodamaged D1 within loops that connect transmembrane helices for PSII repair (Kapri-Pardes et al., 2007; Sun et al., 2007, 2010a; Knopf and Adam, 2018). To investigate a possible role of DEG1C in PSII repair, we exposed control and *DEG1C*-amiRNA lines to photoinhibitory light for 1 h and monitored PSII recovery at low light. As shown in Figure 5A, we found no difference in either the decline of PSII maximum quantum efficiency or the rate at which it recovered. This was also reflected at the level of the D1 protein (Fig. 5B). Hence, the sensitivity of PSII to high light and the ability to repair PSII are not affected in the *DEG1C*-amiRNA line.

Arabidopsis Deg1 has been reported to be involved also in PSII assembly (Sun et al., 2010b). This prompted us to investigate a possible role of DEG1C in PSII biogenesis. To this end, we induced PSII degradation in control and *DEG1C*-amiRNA lines by sulfur starvation for 67 h and monitored the reaccumulation of the D1 subunit of PSII through de novo synthesis upon sulfur repletion for another 24 h (Malnoë et al., 2014; Muranaka et al., 2016). As shown in Figure 5, C and D, there was no significant difference between control and *DEG1C*-amiRNA lines regarding PSII degradation and recovery. In summary, our results suggest that DEG1C does not play a role in either the PSII repair cycle or PSII biogenesis.

As DegP is indispensable for the survival of *E. coli* at elevated temperatures (Lipinska et al., 1989) and DEG1C levels increased under heat stress (Fig. 4A), we reasoned that DEG1C might become important under

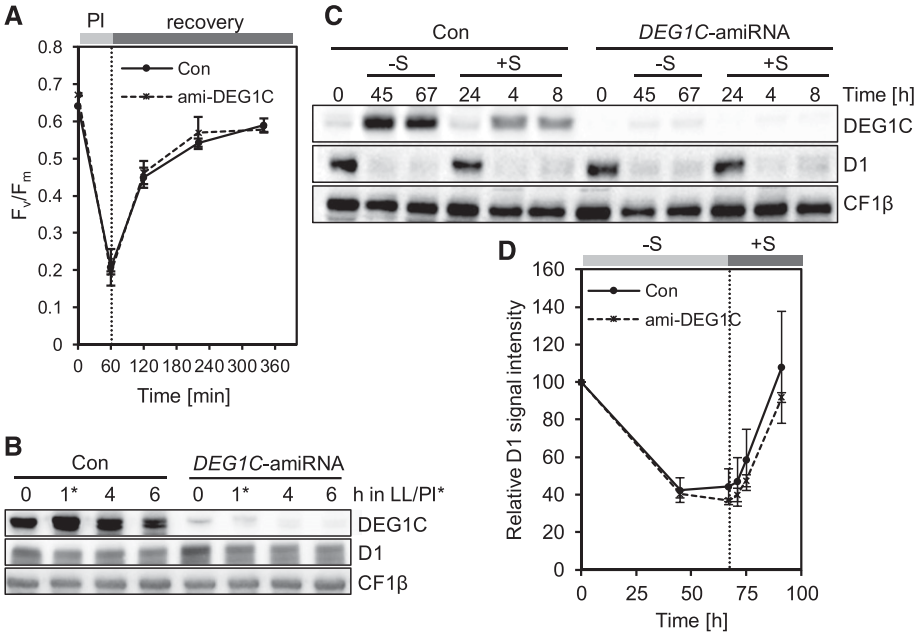

Figure 5. Comparison of control and *DEG1C*-amiRNA lines with respect to their ability to recover PSII from photoinhibition and sulfur starvation. A, cw15-325 control (Con) and *DEG1C*-amiRNA lines were grown in TAP medium at a light intensity of 30 μmol photons m^{-2} s^{-1} to a density of ~3 × 10^6 cells/mL, exposed to 1,800 μmol photons m^{-2} s^{-1} (PI) for 1 h, and allowed to recover at low light (30 μmol photons m^{-2} s^{-1}) for 5 h. PSII maximum quantum efficiency was measured with pulse amplitude-modulated fluorometry. Error bars represent SD, $n = 3$. B, Whole-cell proteins from samples taken during the time course from A were separated on a 12% SDS polyacrylamide gel and analyzed by immunoblotting. CF1β served as a loading control. PI*, time in photoinhibitory light. C, cw15-325 control (Con) and *DEG1C*-amiRNA lines were grown in TAP medium at 30 μmol photons m^{-2} s^{-1} to a density of ~3 × 10^6 cells/mL, harvested by centrifugation, resuspended in TAP-S, and grown for 67 h in TAP-S. After 67 h, the medium was changed back to TAP containing sulfate (+S) and cells were grown for another 24 h under sulfate replete conditions (note that samples from time point 24 h after S repletion were loaded first). Whole-cell proteins (WC) from samples taken during this time course were separated on a 12% SDS polyacrylamide gel and analyzed by immunoblotting. CF1β served as a loading control. D, D1 signal intensities from C were quantified using the FUSIONCapt Advance program. Signals were normalized to the initial D1 levels in each strain. Error bars represent the SD, $n = 3$.

heat-stress conditions. To test this, we measured PSII maximum quantum efficiency and chlorophyll content in control and *DEG1C*-amiRNA lines exposed to 40°C for 6 h. As reported previously by Nordhues et al. (2012), we found a mild decline of PSII maximum quantum efficiency in heat-stressed cells that was, however, indistinguishable between control and *DEG1C*-amiRNA lines (Supplemental Fig. S5A). We found the cellular chlorophyll content to increase slightly (but not significantly) more during heat stress in the *DEG1C*-amiRNA line than in the control line (Supplemental Fig. S5B). Finally, no differences in growth between the two lines were observed on spot tests after 3 h of heat stress at 40°C (Supplemental Fig. S5C). In summary, the depletion of DEG1C had no obvious consequences on the ability of *Chlamydomonas* cells to cope with heat stress.

DEG1C Assembles into Trimers and Hexamers In Vitro and In Vivo

The basic building block of most Deg/HtrA proteases is the trimer, which in the case of bacterial DegP can assemble into a hexamer in the resting state, and into 12-mers and 24-mers in the proteolytically active state (Krojer et al., 2002, 2008; Jiang et al., 2008). Arabidopsis Deg1 exists as monomers that upon activation form trimers that readily convert into proteolytically active hexamers (Chassin et al., 2002; Kley et al., 2011). To analyze the oligomeric state of DEG1C, we separated whole-cell proteins from control and *DEG1C*-amiRNA lines by Blue native PAGE (BN-PAGE) and detected DEG1C by immunoblotting. To improve the detectability of DEG1C complexes and to potentially capture the protease in an active state, cells had been exposed for 3 h to 40°C. As shown in Figure 6A, we detected two protein bands in the wild type that were absent in the amiRNA line and therefore must contain DEG1C. The slower migrating of them migrated at the same position as CDJ1, a cochaperone of chloroplast HSP70. The 40.3-kD protein CDJ1 forms stable dimers that, because of their nonglobular shape, migrate at an apparent mass (~120 kD) much higher than the calculated molecular mass (80.6 kD; Willmund et al., 2008). Given the more globular shape of HtrA trimers, the migration pattern of DEG1C at ~120 kD argues for a trimeric configuration. Hence, DEG1C appears to exist mainly as monomers and trimers in vivo. The depletion of DEG1C in the amiRNA lines had no obvious consequences on the composition of major thylakoid membrane complexes.

To corroborate these findings, we analyzed recombinant DEG1C and whole-cell proteins by BN-PAGE (Fig. 6B). Interestingly, native DEG1C in whole-cell proteins and the recombinant protein displayed the same migration pattern: DEG1C existed as monomers, trimers, and, to a smaller extent, higher-M_r assemblies, presumably hexamers and larger oligomers. Recombinant DEG1C was also treated with dithiobis(succinimidyl propionate) (DSP) to stabilize complexes by crosslinking, or with SDS to destroy formed complexes (Willmund et al., 2008). DSP crosslinking of the recombinant protein enhanced the occurrence of trimers at the expense of monomers, while DEG1C became completely monomeric in the presence of SDS (Fig. 6B). That native and recombinant proteins have the same migration pattern indicates that the recombinant protein behaves like the native one and supports the validity of our in vitro protease assays (Fig. 1; Supplemental Fig. S1).

As a complementary method, we subjected recombinant DEG1C to crosslinking with glutaraldehyde

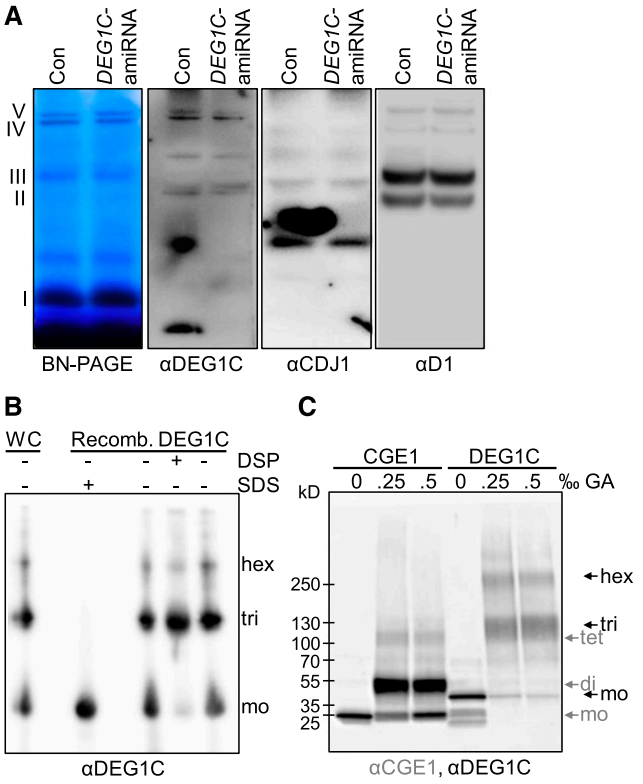

Figure 6. Analysis of the DEG1C oligomeric state. A, Control and *DEG1C*-amiRNA lines in the cw15-325 background were exposed to heat stress at 40°C for 3 h. Cells were solubilized with 1% β-dodecyl maltoside and proteins (equivalent to 5 μg of chlorophyll) separated on a 5% to 15% BN-gel followed by Coomassie staining or immunoblotting. Protein bands in the Coomassie-stained gel were assigned to PSII supercomplexes (V), PSI complexes (IV), PSII monomers (III), CP43-less PSII monomers (II), and LHC trimers (I). B, Two micrograms of purified, recombinant (Recomb.) DEG1C were left untreated, subjected to DSP crosslinking, or incubated with 2% SDS. Samples were separated on a 5% to 12% BN-gel next to β-dodecyl maltoside-solubilized whole-cell proteins (equivalent to 16 μg of chlorophyll) and analyzed by immunoblotting. C, Recombinant CGE1 and DEG1 at a concentration of 1 μM were crosslinked for 10 min with 0%, 0.025%, and 0.05% glutaraldehyde, separated on a 3.5%–10% SDS polyacrylamide gel and analyzed by immunoblotting with antisera against CGE1 and DEG1C. Monomers (mo), dimers (di), and tetramers (tet) formed by CGE1 are depicted with gray letters, and monomers, trimers (tri), and hexamers (hex) formed by DEG1C with black letters.

(GA) and used recombinant CGE1 as a control. Cross-linked protein complexes can be analyzed with standard SDS-PAGE, which allows more reliable estimation of complex masses than BN-PAGE. Corroborating previous work, GA-treated CGE1 migrated at ~27, ~50, and ~110 kD, corresponding to monomers, dimers, and tetramers, respectively (Fig. 6C; Schroda et al., 2001). GA-treated DEG1C migrated at ~40, ~130, and ~260 kD, corresponding to monomers, trimers, and hexamers, respectively.

Lack of DEG1C Affects the Abundance of Proteins Involved in Several Cellular Processes inside and outside the Chloroplast

At this point of our study, we had retrieved an insertional mutant in the *DEG1C* gene from the *Chlamydomonas* library project (CLiP; Li et al., 2016) that harbors the *aphVIII* resistance marker in intron 11 of the *DEG1C* gene (Supplemental Fig. S3C). By direct sequencing of PCR products generated on extracted genomic DNA, we could confirm the cassette insertion site in the *DEG1C* gene locus and the 3′ cassette-genome junction. However, PCRs at the 5′ part of the integration site failed, suggesting a deletion of *DEG1C* gene sequences 5′ to the insertion site (Supplemental Fig. S3D). Accordingly, the DEG1C protein was absent in the mutant and it can therefore be considered as a knock-out mutant (Supplemental Fig. S3E).

To rule out that residual DEG1C protein in *DEG1C*-amiRNA lines concealed phenotypes, we monitored PSII maximum quantum efficiency in the wild type and *deg1c* knock-out mutant exposed to the same high-light and heat-stress regimes employed in Figure 5A and Supplemental Figure S5A, respectively. As we could not detect clear differences between the two strains (Supplemental Fig. S6), we concluded that all targeted analyses to elucidate possible functions of DEG1C in *Chlamydomonas* based on phenotypes observed for Deg homologs in Arabidopsis and bacteria were not successful.

We therefore decided to use an unbiased approach based on quantitative shotgun proteomics to reveal effects of DEG1C depletion at the proteome level. To this end, wild-type and *deg1c* mutant strains were grown for more than ten generations at 25°C and 30 μmol photons m^{-2} s^{-1} in Tris-acetate phosphate (TAP) medium supplemented with $^{15}NH_4Cl$ as the sole nitrogen source, leading to a labeling efficiency of >98%. We then mixed equal amounts of mutant and wild-type cells to generate a universal ^{15}N standard (Mühlhaus et al., 2011). Next, we grew wild-type and *deg1c* mutant cells in TAP medium with $^{14}NH_4Cl$ as a nitrogen source under standard conditions in three replicates. Cells of the ^{15}N universal standard were then mixed with cells from each replicate of wild type and *deg1c* mutant, followed by protein extraction with acetone, tryptic digest, and LC-MS/MS analysis (Fig. 7A). Based on extracted precursor ion chromatograms, the $^{14}N/^{15}N$ ratio was determined for each peptide and combined for multiple peptides of the same protein. By dividing the $^{14}N/^{15}N$ ratio obtained for a protein in the mutant by the $^{14}N/^{15}N$ ratio of that protein in the wild type, we can eliminate the ^{15}N universal standard value from the fraction and get the $^{14}N/^{14}N$ ratio of mutant to wild-type protein. With this approach, potential isotope effects caused by ^{15}N-labeling are eliminated. We identified a total of 1,353 proteins, of which 307 had significantly different abundance in the *deg1c* mutant compared with the wild type ($P < 0.05$; false discovery rate, <0.1). Of these, 115 proteins were of higher abundance and 192 of lower abundance in the *deg1c* mutant compared to the wild type (Fig. 7B; Supplemental Table S1).

At the thylakoid membranes, all subunits of the cytochrome b_6/f complex were more abundant in the *deg1c* mutant, while all subunits of the ATP synthase were less abundant. Of PSI, only subunit E and antenna protein LHCA1 showed elevated levels in the mutant. The pattern for PSII components was more heterogenous: while levels of all three proteins of the oxygen evolving complex, PSBR, and the inner antenna LHCB5 (CP26) were reduced in the mutant, levels of four outer antenna proteins and of LHCSR1 were increased. Moreover, levels of ALB3.2, VIPP1, PSB27, and TEF30, all involved in PSII biogenesis, were elevated in the mutant. This was the case also for FNR1, calcium sensor CAS1, ascorbate peroxidase, and the FTSH1/2 proteases.

In the stroma, five enzymes of the Calvin-Benson cycle had reduced levels in the *deg1c* mutant (note that RBCS2 was quantified based on a single proteotypic peptide that distinguishes RBCS2 from RBCS1. This quantification might be erroneous if this peptide is subject to posttranslational modification). Also, chaperonins CPN60A and CPN60B2, and seven subunits of chloroplast ribosomes were less abundant in the mutant. The picture was less clear regarding chloroplast pathways for fatty acid and tetrapyrrole biosynthesis, where some enzymes were of higher abundance in the mutant and some of lower abundance. Similarly, levels of enzymes involved in both starch synthesis and degradation were elevated (not shown in Fig. 7B; see Supplemental Table S1).

Strikingly, the abundance of many proteins outside of the chloroplast was altered in the *deg1c* mutant when compared with the wild type. Among these proteins were several components of the carbon dioxide concentrating mechanism (CCM), like periplasmic CAH1 and mitochondrial CAH4, which were strongly upregulated in the *deg1c* mutant. This was the case also for chloroplast CCM proteins LCIB/C, CCP1, and LCI11. With an ~17-fold higher abundance, CAH1 was the most strongly differentially regulated protein between the mutant and wild type. Upregulated also were four mitochondrial proteins involved in photorespiration. All other differentially expressed proteins in mitochondria were of lower abundance in the mutant, and these are involved in the tricarboxylic acid cycle and the

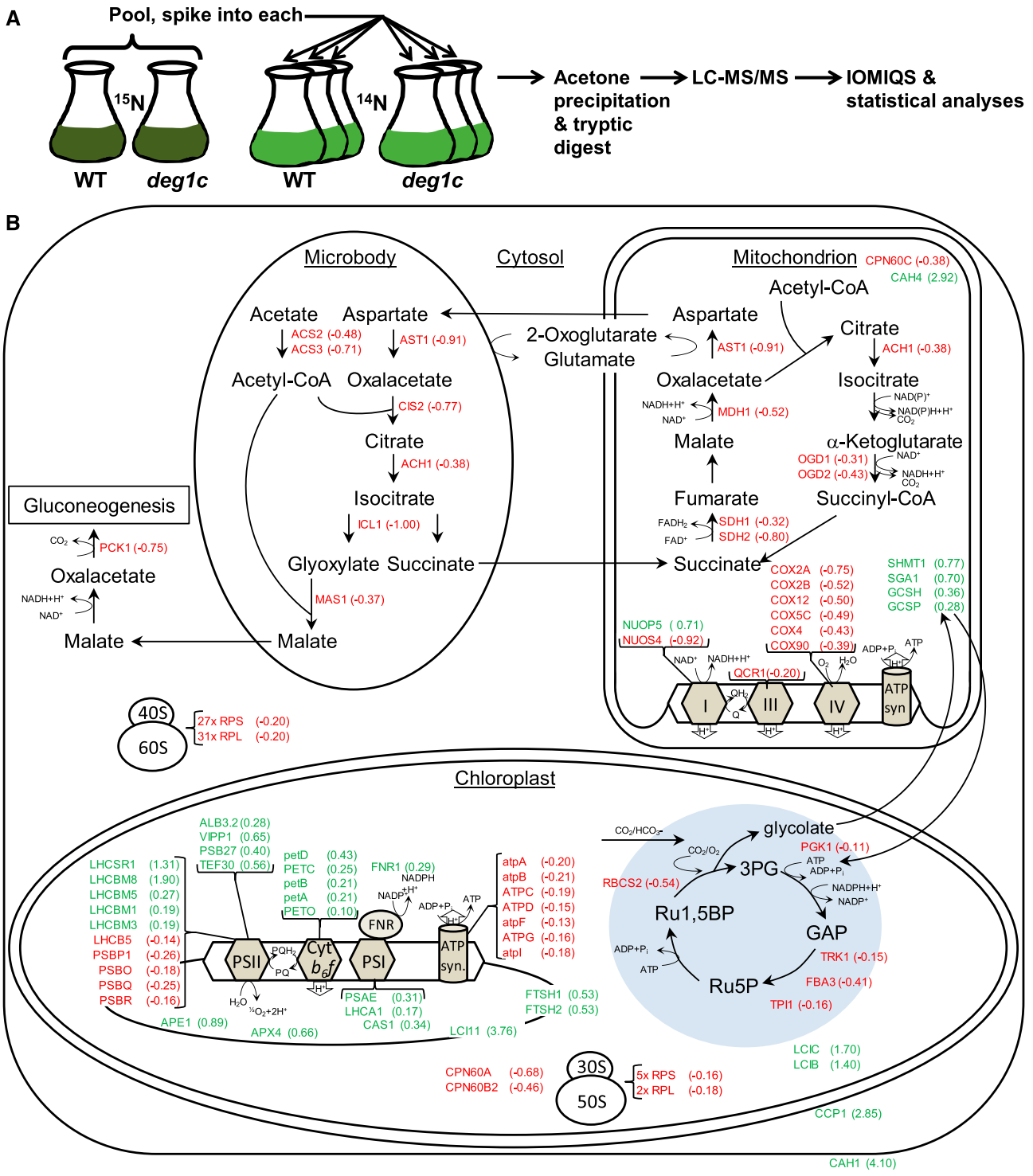

Figure 7. Quantitative shotgun proteomics on the wild type and *deg1c* mutant. A, Workflow for ^{15}N metabolic labeling and mass spectrometry-based quantitative proteomics. IOMIQS, integration of mass spectrometry identification and quantification software. B, Cellular context for 135 of the 307 proteins with altered abundance in the *deg1c* mutant and wild type (Supplemental Table S1) . Proteins with increased abundance are shown in green and those with reduced abundance in red. Values indicate mean log2-transformed fold changes from three biological replicates. Enzymes of the glyoxylate and tricarboxylic acid cycle: ACS2/ACS3, Acetyl-CoA synthetase; AST1, Asp aminotransferase; CIS2, glyoxysome citrate synthase; ACH1, aconitate hydratase; ICL1, isocitrate lyase; MAS1, malate synthase; OGD1/2, 2-oxoglutarate dehydrogenase; SDH1/2, succinate dehydrogenase; MDH1, malate dehydrogenase. Photorespiration: SHMT, Ser hydroxymethyltransferase; SGA1, Ser-glyoxylate aminotransferase; GCSH and GCSP, Gly decarboxylase subunits. Gluconeogenesis: PCK1, phosphoenolpyruvate carboxykinase. Components of

respiratory chain (NUOP5 might be misannotated). Several cytosolic and glyoxysomal enzymes involved in acetate assimilation and gluconeogenesis were also downregulated in the *deg1c* mutant, as were levels of 58 subunits of cytosolic ribosomes.

To verify differential protein accumulation between the wild type and *deg1c* mutant, we detected levels of selected proteins for which we had antisera available by immunoblotting. As shown in Figure 8A, we could verify increased levels of VIPP1/2 and LCIB and slightly decreased levels of OEE2 and CF1β in the *deg1c* mutant. This protein accumulation pattern was also observed in a *DEG1C*-amiRNA line, indicating that it is caused by the depletion of the DEG1C protease and not by a secondary mutation in the *deg1c* mutant line. This conclusion is further supported by increased levels of LHCSR1 and slightly reduced levels of CPN60 and CF1β in a *DEG1C*-amiRNA line of another strain background.

The Physiology of Photosynthesis Is Not Changed in the *deg1c* Mutant under Nonstress Conditions

We wondered whether the observed differential accumulation of photosynthetic subunits in the *deg1c* mutant affects the photochemical rate. For this, we monitored the electrochromic shift (ECS) of photosynthetic pigments (Witt, 1979), which corresponds to the change in the absorption spectrum of some photosynthetic pigments in response to the electric field generated by the activity of photosynthetic complexes. Under steady-state illumination, the electric field generated by the photosynthetic activity is constant. When light is switched off, the two photosystems instantaneously stop producing charge separations, whereas other complexes (not using light as substrate) keep on working at the same rate for a few milliseconds. The initial rate of the ECS decay is therefore a measure of the rate at which the photosystems performed charge separations in the light, i.e. the photochemical rate (Bailleul et al., 2010). With this method, we found no difference in the light dependency of the electron transfer rates between wild type and *deg1c* mutant (Supplemental Fig. S7A). Values were similar between the wild type and mutant for the light saturation parameter, E_k (Supplemental Fig. S7B), and the maximal photochemical rate, V_{max} (Supplemental Fig. S7, B and D), indicating that there was no difference in either the efficiency to capture light or the limiting step of photosynthesis.

To test potential differences in cyclic electron flow (CEF), we measured the photochemical rate when PSII was inhibited with saturating concentrations of 3-(3,4-dichlorophenyl)-l,l-dimethylurea. Under these conditions, only PSI can perform charge separations and the only possible mode of electron transfer is CEF. We found no significant difference in CEF rates between the *deg1c* mutant and the wild type (Supplemental Fig. S7C). However, the rate of CEF measured when PSII is inhibited can be different from that present under physiological conditions (Fan et al., 2007). Therefore, these measurements should be interpreted with caution.

To assess possible changes in the ratio of the two photosystems in the mutant, we compared the ECS signal produced by a single-turnover flash of saturating intensity when the two photosystems are active with that obtained when only PSI is active, i.e. after inhibition of PSII with 3-(3,4-dichlorophenyl)-l,l-dimethylurea and hydroxylamine. The PSII/PSI ratio was ~20% higher in the *deg1c* mutant when compared with the wild type (Fig. 8B).

Proteomics revealed a nearly 12% lower abundance of chloroplast ATP synthase in the *deg1c* mutant versus the wild type. Therefore, we also measured the ECS decrease kinetics when turning off the light after a saturating light pulse. Under these experimental conditions, the electric field measured by ECS is dissipated by the ATP synthase activity, and possibly by other sources of membrane electric permeability (Joliot and Joliot, 2008). The kinetics of ECS decrease were the same in the *deg1c* mutant and wild type (Supplemental Fig. S8), ruling out differences in ATP synthase activity or membrane permeability.

In the absence of light and photosynthetic activity, the electrochemical proton gradient across the thylakoid membrane ($\Delta\mu H+$) is in equilibrium with the intracellular ATP/ADP ratio due to the reversible activity of the ATP synthase. With the maximal reachable value

Figure 7. (*Continued.*)
mitochondrial respiratory chain complexes: COX, Cytochrome c oxidase subunits (complex IV); QCR1, ubiquinol:cytochrome c oxidoreductase subunit (complex III); NUO, NADH:ubiquinone oxidoreductase subunits. Cytosolic 80S ribosome: averages from 31 large (RPL) and 27 small (RPS) subunits. Carbon dioxide concentrating mechanism: CAH, carbonic anhydrase; LCIB/C/11, low-CO_2 inducible protein; CCP1, low-CO_2-inducible chloroplast envelope protein. Photosynthetic electron transport chain: PSAE, PSI reaction center subunit E; LHCA1, light-harvesting protein of PSI; LHCB, chlorophyll a/b binding proteins of LHCII; LHCSR1, stress-related chlorophyll a/b binding protein; PSBR, R subunit of PSII; PSBQ/O/P1, oxygen-evolving enhancer proteins of PS II. Thylakoid membrane protein complex biogenesis factors: ALB3, albino; VIPP1, vesicle inducing protein in plastids; PSB27, PSII assembly factor; TEF30, thylakoid enriched fraction; PET, cytochrome b_6f complex subunits; FNR1, ferredoxin-NADP reductase; ATP, chloroplast ATP synthase subunits. Other thylakoid proteins: CAS1, calcium sensor receptor; APX4, ascorbate peroxidase; APE1, acclimation of photosynthesis to the environment; FTSH, filamentation temperature-sensitive. Calvin-Benson cycle enzymes: RBCS2, Rubisco small subunit; PGK1, phosphoglycerate kinase; TRK1, transketolase; FBA3, Fru-1,6-bisphosphate aldolase; TPI1, triose phosphate isomerase; CPN60, chaperonins. Chloroplast 60S ribosome: averages from two large (RPL) and five small (RPS) subunits.

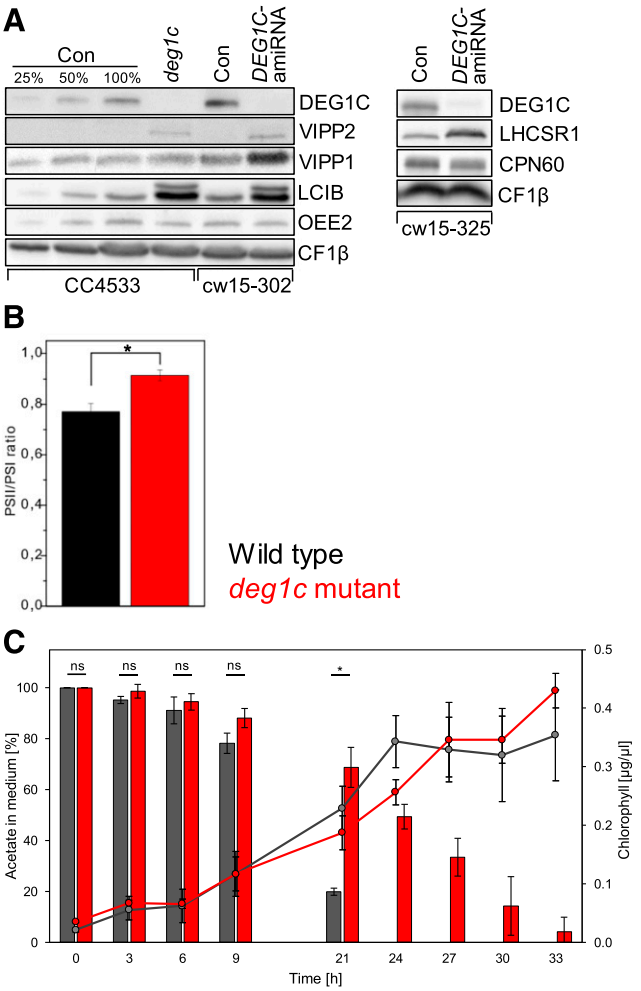

Figure 8. Validation of results from quantitative shotgun proteomics. A, Analysis of the accumulation of selected proteins in control (Con) lines, the *deg1c* knock-out mutant and two *DEG1C*-amiRNA lines grown at 25°C and 30 μmol photons m^{-2} s^{-1}. The control in the CC4533 background is the CLiP parent strain (Li et al., 2016). In strain backgrounds cw15-302 and cw15-325, the controls are transformants generated with the *ARG7* wild-type gene alone. B, Comparison of PSII/PSI ratio between the wild type (black) and the *deg1c* mutant (red). C, Analysis of acetate consumption in relation to growth of the wild type (dark gray) and *deg1c* mutant (red). Both strains were inoculated in the same batch of TAP medium at an OD750 of 0.1 and grown at 25°C and 30 μmol photons m^{-2} s^{-1}. The first sample was taken after 2 h ($t = 0$). The acetate left in the medium is represented as bars indicating the percent of the original concentration (1 g/L), and chlorophyll concentrations are given as circles. Error bars represent the SD, with $n = 3$, and asterisks indicate significant differences between the wild type and *deg1c* mutant (Student's t test, $^*P < 0.01$). ns, not significant.

of the electric field across thylakoids as a reference (ions leak when it exceeds the electric permeability of the membrane; Joliot and Joliot, 2008), the amplitude of the ECS increase during a saturating light pulse is inversely correlated to the dark value of the $\Delta\mu H+$. Since we found no difference between *deg1c* mutant and wild type regarding the amplitude of the ECS created during a saturating light pulse (Supplemental Fig. S8), the $\Delta\mu H+$ and the chloroplast ATP/ADP ratio in the dark must be similar in the two strains.

The *deg1c* Mutant Exhibits Slower Rates of Acetate Consumption than the Wild Type

The surprising down-regulation of proteins of the glyoxylate cycle, the tricarboxylic acid cycle, and the mitochondrial respiratory chain in the *deg1c* mutant versus the wild type implicated a reduced capacity of the mutant to use the acetate in the medium. To test this, we grew the *deg1c* mutant and the corresponding wild type in TAP medium at 25°C and 30 μmol photons m^{-2} s^{-1}, i.e. under mixotrophic growth conditions, and measured the concentration of acetate in the medium over time. In parallel, we measured the chlorophyll concentration in the cultures as a proxy for cell density, because cells of CLiP strains tend to form clumps and are difficult to count. As shown in Figure 8C, there was already a trend toward reduced acetate consumption in the mutant during the first 9 h of cultivation, but there was no effect on growth. After 24 h of cultivation, however, the wild type had used up the acetate in the medium, while in the *deg1c* mutant ~50% of the acetate was still left. At this time, the wild type had reached the stationary phase and its cell density was higher than that of the mutant. It took the mutant 3 h more to reach this density. Interestingly, in the following 6 h, the *deg1c* mutant continued to grow to cell densities above those of the wild type at the stationary phase and apparently achieved this by using up the remaining acetate in the medium.

DISCUSSION

We report on the molecular and biochemical characterization of DEG1C, one of 15 Deg/HtrA proteins encoded by the *Chlamydomonas* genome (Schroda and Vallon, 2009; Schuhmann et al., 2012). With one protease domain containing the canonical Asp-His-Ser catalytic triad, and one PDZ domain, DEG1C shares a similar domain structure with DegS in the bacterial periplasm, human HtrA proteins with various localizations, and Arabidopsis Deg1 in the thylakoid lumen (Supplemental Fig. S9; Clausen et al., 2002). DEG1C efficiently degraded unfolded model substrates like casein, MDH, lysozyme, or BSA (Fig. 1; Supplemental Fig. S1) and, like Arabidopsis Deg1, is in a dynamic equilibrium between monomers, trimers, and hexamers (Fig. 6; Chassin et al., 2002; Kley et al., 2011). The proteolytic activity of DEG1C increased at temperatures of 37°C and above, presumably because higher temperatures promote substrate unfolding (Kolmar et al., 1996; Kim et al., 1999; Chassin et al., 2002; Ge et al., 2014). Accordingly, at these temperatures the chloroplast small heat shock proteins HSP22E and HSP22F were found to accumulate and to integrate into forming protein aggregates (Rütgers et al., 2017b). Under standard growth

conditions, we estimated a DEG1C concentration of 0.45 μM in the chloroplast, and with this DEG1C accumulates to about 9-fold and 2.5-fold lower levels than two major chloroplast chaperone machineries, HSP70B/CDJ1 and HSP90C, respectively (Willmund and Schroda, 2005; Willmund et al., 2008).

Despite Being Orthologs, Arabidopsis Deg1 and *Chlamydomonas* DEG1C Localize to Different Sides of the Thylakoid Membrane

Chlamydomonas DEG1A, DEG1B, and DEG1C are orthologous to Arabidopsis Deg1 and are likely the result of gene duplications that occurred after the divergence of the common ancestor of green algae and land plants (Schroda and Vallon, 2009; Schuhmann et al., 2012). To get an estimate of the abundance of these three proteins and the other predicted *Chlamydomonas* chloroplast Deg1 family members in the stroma (DEG2 and DEG7) and thylakoid lumen (DEG5 and DEG8), we consulted seven previous studies in which *Chlamydomonas* cells had been exposed to various environmental conditions and isolated chloroplasts and/or entire cells analyzed by shotgun proteomics (Terashima et al., 2010; Mühlhaus et al., 2011; Höhner et al., 2013; Plancke et al., 2014; Ramundo et al., 2014; Park et al., 2015; Schroda et al., 2015). DEG1C was the only of these seven proteins that was detected in all studies and always had the highest peptide coverage, indicating that DEG1C is the major chloroplast Deg family member in *Chlamydomonas*. DEG1A was detected in four studies and DEG5, DEG7, and DEG8 in two studies each, while DEG1B and DEG2 were never detected. These data, and the finding that DEG1B in *Volvox* lacks the Asp residue in the catalytic triad (Supplemental Fig. S9), point to a minor role for DEG1B, which nevertheless is expressed in *Chlamydomonas* (Fig. 2; Supplemental Fig. S2).

Like Deg1 from land plants, DEG1A proteins from *Chlamydomonas* and *Volvox* contain putative targeting signals for the chloroplast Sec pathway at their N termini, which are missing in DEG1C sequences from *Chlamydomonas* and *Volvox* (Supplemental Fig. S9). Accordingly, we found that *Chlamydomonas* DEG1C localized to the stroma and the stromal side of thylakoid membranes (Fig. 3), while Arabidopsis Deg1 localizes to the lumen and the lumenal side of thylakoid membranes (Itzhaki et al., 1998; Sun et al., 2007). These different localizations are also supported by the different pH optima for proteolytic activity, which lie at pH 6 for Deg1 (Chassin et al., 2002; Kley et al., 2011) and at pH 8 for DEG1C (Fig. 1F; Supplemental Fig. S1C) and therefore match the prevailing pH values in lumen and stroma, respectively. His-244 was identified as the pH-sensing residue in Deg1 (Kley et al., 2011), and this residue is also conserved in DEG1C sequences (Supplemental Fig. S9). Presumably, in the presence of substrates, Deg1 turns into the proteolytically active form after protonation of His-244 (Kley et al., 2011). In contrast, deprotonation of that residue appears to be required to turn DEG1C into the active form, as proteolytic activity of DEG1C strongly increased at pH values >6 (Fig. 1F; Supplemental Fig. S1C).

In Contrast to Arabidopsis Deg1, *Chlamydomonas* DEG1C Plays No Important Role in PSII Biogenesis and Repair

On both sides of the thylakoid membrane, chloroplast Deg proteases from streptophytes have been implicated in the degradation of photosynthetic proteins, especially photodamaged D1, as a first step of the PSII repair cycle (Kapri-Pardes et al., 2007; Sun et al., 2007, 2010a; Zienkiewicz et al., 2012; Knopf and Adam, 2018). Arabidopsis *deg1* knock-down mutants were retarded in growth already under standard growth conditions and this was attributed to the reduced accumulation of PSII supercomplexes and the resulting lower quantum yield of PSII (Sun et al., 2010b). Based on this observation and the finding that Deg1 interacted with the D2 protein, the authors also suggested a chaperone role for Deg1 in PSII assembly. In the Arabidopsis *deg1* knockout mutant, the abundance of all complexes of the photosynthetic light reactions was reduced by 15% to 30% (Butenko et al., 2018).

Under standard conditions (25°C and 30 μmol photons m^{-2} s^{-1}), PSII was photochemically fully functional in *Chlamydomonas* lines depleted of DEG1C. Moreover, the sensitivity of PSII to photodamage and the rate of PSII repair were indistinguishable between DEG1C depleted lines and control lines (Fig. 5, A and B; Supplemental Fig. S6A). Therefore, DEG1C appears not to be involved in PSII repair. Also, we found no significant effect in DEG1C-depleted lines on the rates of PSII degradation following sulfur starvation, or on the rates of PSII resynthesis after sulfur repletion (Fig. 5, C and D). This is surprising, as the highest accumulation of DEG1C (17.5-fold) was observed upon sulfur starvation (Fig. 4G). Similarly, heat stress, leading to a >4.7-fold increase in accumulation of DEG1C (Fig. 4G), did not cause any obvious phenotypes at the level of PSII maximum quantum efficiency, chlorophyll content, or survival in DEG1C depleted lines (Supplemental Fig. S5). Possibly, a role in D1 degradation is carried out by DEG1A or DEG1B, the two other *Chlamydomonas* orthologs of Arabidopsis Deg1, presumably supported by stromal DEG7 similar to its ortholog in Arabidopsis (Sun et al., 2010a).

Downregulation of Proteins Involved in Various Cellular Processes in the *deg1c* Mutant Has Virtually No Consequences for Cell Physiology, Pointing to an Excess of These Proteins

Quantitative shotgun proteomics allowed us to detect changes in the abundance of 307 proteins between the *deg1c* mutant and wild type under standard growth conditions (Fig. 7B; Supplemental Table S1). Among the 192 proteins of reduced abundance were several enzymes of the Calvin-Benson cycle and the glyoxylate

cycle, with up to 50% lower levels of isocitrate lyase. In line with the reported key role of this enzyme in acetate metabolism (Plancke et al., 2014), we observed a reduced uptake of acetate in the *deg1c* mutant (Fig. 8C). However, this had surprisingly little consequence on the growth rate, presumably because the mutant could better exploit CO_2 as a carbon source via the CCM. The 10% to 13% reduced abundance of 65 subunits of cytosolic and chloroplast ribosomes in the *deg1c* mutant apparently also had no strong effects on growth.

Although the abundance of protein components of the tricarboxylic acid cycle, the mitochondrial respiratory chain, and the chloroplast ATP synthase was reduced in the *deg1c* mutant, we observed no difference in ATP/ADP ratios in the dark between it and the wild type (Supplemental Fig. S8). This suggests that either ATP synthesis through respiration was not affected or ATP consumption was reduced in the *deg1c* mutant. Also, we detected no changes in the chloroplast ATP synthase activity in the mutant.

The lack of a photosynthetic electron flow phenotype even upon diminution of the abundance of some enzymes by up to 50% indicates that there is an excess capacity for these enzymes in *Chlamydomonas*. Accordingly, *Chlamydomonas* mutants with Rubisco levels reduced by up to 50% of wild-type levels have been reported to exhibit wild-type-like phototrophic growth (Johnson, 2011). Similarly, a 20% to 50% lower abundance of the cytochrome b_6/f complex did not alter phototrophic growth of *Chlamydomonas* (Chen et al., 1995). Hence, it appears that *Chlamydomonas* can invest anabolic capacities in some pathways at the expense of other pathways without significant effects on basic cell physiology.

The Most Strongly Upregulated Proteins in the *deg1c* Mutant Are Characteristic of an Acclimation Response to High Light

Among the 115 proteins with increased abundance in the *deg1c* mutant were several proteins typically involved in acclimation to high light intensities, despite growth under low light (30 μmol photons m^{-2} s^{-1}). These proteins represent the most strongly upregulated ones in the mutant (Fig. 7; Supplemental Table S1). They comprise enzymes of the CCM and photorespiration, both providing additional electron sinks (Wingler et al., 2000; Yamano et al., 2008); two ascorbate peroxidases involved in antioxidant defense (Caverzan et al., 2012); proteins with roles in photoprotection (LHCBM8; Girolomoni et al., 2017) and the transfer of excitation energy to PSI (LHCSR1; Kosuge et al., 2018); and a homolog of the Arabidopsis APE1 protein involved in acclimation to high light (Walters et al., 2003). Since most of these upregulated proteins are not localized in the stroma, they cannot be substrates of DEG1C and must be upregulated via signaling pathways responding to decreased DEG1C activity. Note that in the Arabidopsis *deg1* mutant, proteins involved in photoprotection were upregulated as well (Butenko et al., 2018).

The question arises as to what could have triggered a high light acclimation response at low light intensities in DEG1C-depleted lines? Unfortunately, we can only speculate here. One idea is that the response is due to the 20% higher ratio of active PSII versus PSI estimated by electrochromic shift experiments (Fig. 8B). As the core subunits of PSII and PSI were equally abundant in *deg1c* mutant and wild type (Fig. 7B; Supplemental Table S1), we suggest that a small fraction of PSI is not active. This could lead to an over-reduced plastoquinone pool, through which the high light acclimation response is triggered.

Another idea is that misfolded and unassembled proteins accumulate in thylakoid membranes of DEG1C-depleted lines as a result of reduced quality control and clearance activity. A role of DEG1C in protein quality control at the thylakoid membrane would make sense considering its high proteolytic activity and its preference for unfolded proteins (Fig. 1; Supplemental Fig. S1). Impaired protein quality control at thylakoid membranes might be alleviated, but not fully compensated, by the upregulation of the membrane-intrinsic FtsH protease by ~45%. In the Arabidopsis *deg1* mutant, FtsH proteases were upregulated as well (Butenko et al., 2018). In the wild type, high light conditions could induce the accumulation of misfolded and unassembled proteins through an increased rate of PSII repair and through protein oxidation. Therefore, misfolded and unassembled proteins, accumulating in DEG1C-depleted lines also under low light conditions, might be sensed directly and "interpreted" by the cell to be a result of high light damage. Alternatively, misfolded and unassembled proteins can cause lipid packing defects, which may result also from high light-induced lipid peroxidation (Wong-Ekkabut et al., 2007; McDonald et al., 2015). In this case, lipid packing defects could be sensed and interpreted to be a result of high light damage. At bacterial plasma membranes, lipid packing defects are sensed by the phage shock protein A (PspA), which activates a transcription factor to increase its own expression and, after forming large homo-oligomers, binds to the membrane to fix the defects (Jovanovic et al., 2014; McDonald et al., 2015, 2017). A similar role has been reported for VIPP1, a relative of PspA in the chloroplast, under oxidative and osmotic stress conditions (Zhang et al., 2012, 2016). That a similar process might be at work in DEG1C-depleted lines is supported by the finding that they upregulated VIPP1 and VIPP2 (Figs. 7 and 8). Both proteins, as well as DEG1C, were also upregulated upon depletion of the ClpP protease (Ramundo et al., 2014).

The accumulation of misfolded and unassembled proteins and/or the resulting lipid packing defects in the thylakoid membranes of DEG1C-depleted lines might also impair the translocation and integration of thylakoidal proteins via the twin-arginine translocation, Sec, and ALB3 pathways, with strongest effects on the import of abundant proteins like the oxygen-evolving

complex subunits of PSII. This could account for their mild reduction of up to 17% in the *deg1c* mutant when compared with the wild type (Figs. 7 and 8). Presumably as a compensation, levels of factors involved in PSII biogenesis and repair, i.e. ALB3 (Göhre et al., 2006), VIPP1 (Nordhues et al., 2012; Walter et al., 2015), PSB27 (Roose and Pakrasi, 2008), and TEF30 (Muranaka et al., 2016), were increased by up to 56% in the mutant. This is in line with the upregulation of photosystem biogenesis and repair factors in the Arabidopsis *deg1* mutant, including TATB, ALB3, Y3IP1, and LPA2, which was also interpreted as a compensating response (Butenko et al., 2018).

The relatively low impact on cellular homeostasis upon depletion of DEG1C points to a high effectiveness of the compensating responses and to the robustness of the chloroplast protein quality control network.

MATERIALS AND METHODS

Strains and Cultivation Conditions

Chlamydomonas reinhardtii wild-type CC-4533 and *deg1c* knock-out strain LMJ.RY0402.139586 from CLiP (Li et al., 2016) and strain CC-124 were obtained from the *Chlamydomonas* Resource Center. Strain CF185 is described in Schroda et al. (1999). Strains cw15-325 and cw15-302 (cw_d, mt^+, $arg7^-$), kindly provided by René Matagne (University of Liège, Belgium), were used as recipient strains for transformation with plasmid pCB412 (containing only the *ARG7* gene), or with pMS668 (containing the *ARG7* gene and the *DEG1C*-amiRNA construct). Cultures were grown mixotrophically in TAP medium (Kropat et al., 2011) on a rotatory shaker at 25°C and ~30 μmol photons m^{-2} s^{-1}. Cell densities were determined using a Z2 Coulter Counter (Beckman Coulter). Acetate concentrations in the medium were analyzed as described previously (Rohr et al., 2019).

Cloning, Expression, and Purification of Recombinant DEG1C

The *DEG1C* coding sequence was amplified by PCR from *Chlamydomonas* complementary DNA (cDNA) with primers 5′-CACGCCCAGCTCTTCGAA CGCGGCAGATCTGACGGCGCC-3′ and 5′-GCGTCTCGAGCCATTACTCA GTCACATTGA-3′. The resulting 1,187-bp PCR product was digested with SapI and *Xho*I and cloned into SapI/*Xho*I-digested pTYB11 (New England Biolabs), yielding pMS686. DEG1C was expressed as a fusion protein in *Escherichia coli* ER2566 and purified by chitin affinity chromatography according to the manufacturer's instructions (New England Biolabs). Eluted DEG1C was concentrated in Amicon Ultra-15 centrifugal filter devices (Millipore) and dialyzed against KMH buffer (20 mM HEPES-KOH, pH 7.2, 80 mM KCl, and 2.5 mM $MgCl_2$). Purified proteins were frozen in liquid nitrogen and stored at −80°C.

Protease Activity Assays

Purified DEG1C (1.3 μM) was incubated in a total volume of 100 μL of 50 mM HEPES (pH 7.4) with model substrates (13 μM) at 40°C for 2 h, unless indicated otherwise. As substrates, casein (Roth), porcine heart MDH (Sigma), egg white lysozyme (Roche), and BSA (Sigma) were used. To induce (partial) protein unfolding, reactions containing lysozyme and BSA were supplemented with 2 mM DTT final concentration.

Protein Analyses

For whole-cell protein extraction, cells were pelleted and resuspended in 75 mM Tris-HCl, pH 6.8, 2% (w/v) SDS, and 10% (v/v) glycerol, boiled at 96°C, and centrifuged. After protein quantification according to Lowry et al. (1951), Laemmli buffer (Laemmli, 1970) was added and proteins were subjected to SDS-PAGE and semidry blotting on nitrocellulose membranes as described previously (Schroda et al., 1999). BN-PAGE with whole-cell proteins was carried out according to published protocols (Schägger and von Jagow, 1991; Schägger et al., 1994), with minor modifications. Briefly, ~1×10^8 cells were harvested by centrifugation, washed with TMK buffer (10 mM Tris-HCl, pH 6.8, 10 mM $MgCl_2$, 20 mM KCl), and resuspended in 500 μL ACA buffer (750 mM ε-aminocaproic acid, 50 mM Bis-Tris pH 7.0 and 0.5 mM EDTA) supplemented with 0.25× protease inhibitor (Roche). Cells were broken by sonication. Intact cells and cell debris were removed by centrifugation for 15 min at 300*g* and 4°C. Whole-cell lysates (equivalent to 0.25 μg/μL of chlorophyll) were solubilized for 15 min with 1% (w/v) β-dodecyl maltoside (Roth) on ice in the dark, and insolubilized material was precipitated at 14,000*g* for 15 min at 4°C. Afterward, supernatants were supplemented with native sample buffer (Bio-Rad) and separated on 5% to 15% (w/v) or 5% to 12% (w/v) BN polyacrylamide gels. BN-PAGE of recombinant protein was done with 2 μg of purified, recombinant DEG1C, as described previously (Willmund et al., 2008). For in vitro crosslinking, recombinant protein in 50 mM Bis-Tris, 15% (w/v) glycerol, 1 mM $MgCl_2$, and 80 mM KCl was supplemented with 200 mM dithio-bis(succinimidyl propionate) (DSP) and incubated for 30 min at 25°C. Crosslinking was quenched by adding ε-aminocaproic acid at a final concentration of 0.4 M and incubating for 15 min at 25°C. Antisera used were against HSP90C (Willmund and Schroda, 2005), CGE1 (Schroda et al., 2001), VIPP1 (Liu et al., 2005), CF1β (Lemaire and Wollman, 1989), mtCA (Agrisera AS11 1737), cytochrome *f* (Pierre and Popot, 1993), PsaA (Agrisera AS06 172), PsbA (Agrisera AS05 084), SecA (M. Schroda, unpublished data), PsaN (M. Schroda, unpublished data), cpRPL1 (Ries et al., 2017), CPN60B2 (Rütgers et al., 2017a), and LHCSR1 (Agrisera AS14 2819). Anti-rabbit-HRP (Sigma-Aldrich) was used as secondary antibody in a 1:10,000 dilution. Immunodetection was performed using enhanced luminol-based chemiluminescence detected with the FUSION-FX7 Advance imaging system, and band quantifications after immunodetections were done using the FUSIONCapt Advance program (PeqLab).

Immunofluorescence Microscopy

For immunofluorescence microscopy, cells were fixed and stained as described previously (Uniacke et al., 2011), with minor modifications. Briefly, microscopy slides were given two 10 min washes in 100% ethanol. To enhance adherence of the cells to the slides, slides were coated with 0.1% (v/v) poly-L-Lys. Cells were fixed with 4% (v/v) formaldehyde for at least 2 h at 25°C on an overhead rotator. Aliquots of 40 μL cell suspension were allowed to adhere to the microscope slides for 7 min at 25°C, followed by incubation in 100% methanol for 6 min at −20°C. Afterward, slides were washed three times with phosphate-buffered saline (PBS) for 5 min each. Cell permeabilization was achieved by incubating the slides with 2% (v/v) Triton X-100 in PBS for 10 min at 25°C. Additionally, slides were washed in PBS-Mg (PBS and 5 mM $MgCl_2$) three times and blocked with PBS-BSA (PBS and 1% [w/v] BSA) for at least 30 min at 25°C. Slides were incubated overnight at 4°C in primary antisera against DEG1C or HSP90C in 1:2,500 and 1:4,000 dilutions in PBS-BSA, respectively. Slides were then washed twice in PBS for 10 min at 25°C, followed by incubation in a 1:200 dilution of the fluorescein isothiocyanate-labeled goat anti-rabbit antibody (Sigma-Aldrich) in PBS-BSA for 2 h at 25°C. Finally, the slides were washed three times with PBS for 5 min each and mounting solution containing 4′,6-diamidino-2-phenylindole (DAPI; Vectashield, Vector Laboratories) was dispersed over the cells. Images were captured with an Olympus BX53 microscope with filters for DAPI and fluorescein isothiocyanate and an Olympus DP26 color camera.

Heat Shock, Oxidative Stress, and Sulfur-, Nitrogen-, and Phosphorus-Starvation Experiments

For the heat-stress experiment, exponentially growing cells were pelleted by centrifugation at 25°C and 1,000*g* for 2 min, resuspended in TAP medium prewarmed to 42°C, and incubated in a 42°C water bath under agitation and constant illumination at ~40 μmol photons m^{-2} s^{-1}. High light and photoinhibition treatments were performed as described previously (Nordhues et al., 2012). Light intensities were determined using a Luxmeter (Walz). For sulfur-, phosphorus-, and nitrogen-starvation experiments, cells were pelleted by centrifugation at 25°C and 1,000*g* for 2 min, washed twice in TAP medium deprived of sulfur (TAP-S), phosphorus (TAP-P) or nitrogen (TAP-N) and resuspended in TAP-S, TAP-P, or TAP-N, respectively. Sulfur repletion was performed by pelleting the cells as described above and resuspending them in regular TAP medium.

Cell Fractionations and Trypsin Treatment

Crude fractionation of cells into soluble and membrane fractions, salt wash, and trypsin treatment were performed as described previously (Muranaka et al., 2016) but using 0.0625 mg mL^{-1} trypsin. Isolation of chloroplasts and subfractionation into stroma and thylakoids was done according to Zerges and Rochaix (1998). Mitochondria were isolated as described by Eriksson et al. (1995), but using a BioNebulizer (Glas-Col) for cell disruption.

Affinity Purification of DEG1C Antibodies

About 1 mg of recombinant DEG1C protein was separated onto an SDS gel, transferred by semidry blotting onto a nitrocellulose membrane, and stained with Ponceau S. The area containing the DEG1 protein was cut out and the resulting membrane piece incubated for 10 min in a 2-mL tube with a solution containing 100 mM Gly at pH 2.5. The membrane piece was then washed with PBS containing 0.1% (v/v) Tween 20 (PBS-T) and incubated under agitation for 1 h at 25°C in PBS-T containing 3% (w/v) milk powder. Following three washes with PBS-T, the membrane piece was incubated under agitation overnight at 4°C with 1.5 mL polyclonal antiserum against DEG1C. After three washes with PBS-T, bound antibodies were eluted by incubating twice for 2 min with 2 mL 100 mM Gly, pH 2.5 solution. Then, 1-mL aliquots of the eluate were transferred into a tube already containing 75 μL of 2 M Tris-HCl, pH 8.5. Successful neutralization was verified with lackmus paper. Purified antibodies were supplemented with 0.02% (w/v) sodium azide and stored at −80°C.

Immunoprecipitation from Soluble Cell Extracts

Chlamydomonas cells were harvested by centrifugation at 1,000*g* and 4°C, resuspended in 1 mL lysis buffer (20 mM HEPES-KOH, pH 7.2, 10 mM KCl, 1 mM $MgCl_2$, 154 mM NaCl, and 0.25× protease inhibitor cocktail [Roche]). Cells were broken by freezing/thawing and centrifuged for 30 min at 4°C and 18,000 g. The supernatant was supplemented with 0.5% (v/v) Triton X-100 final. Soluble fractions were incubated with 50 μL of protein A-Sepharose beads coupled with the polyclonal antibody against DEG1C as described previously (Schroda et al., 2001). Immunoprecipitation was carried out for 1 h at 4°C on an overhead rotator. Afterward, beads were washed with lysis buffer six times and twice with 10 mM Tris-HCl, pH 7.0. Elution of proteins was achieved by boiling the samples in Laemmli buffer lacking DTT at 95°C for 5 min. Eluates were supplemented with 0.1 M DTT, separated by SDS-PAGE, and silver stained, and protein bands were cut out and analyzed by LC-MS/MS.

Chlorophyll Fluorescence Measurements

Maximum quantum efficiency of PSII (F_v/F_m) was measured using a pulse amplitude-modulated Mini-PAM fluorometer (Heinz Walz) essentially according to the manufacturer's protocol after 3 min of dark adaptation (1-s saturating pulse of 6,000 μmol photons m^{-2} s^{-1}, gain = 4).

Vector Construction and Screening for DEG1C-Underexpressing Transformants

The artificial microRNA targeting *Chlamydomonas* DEG1C was designed with the WMD2 Web tool (Ossowski et al., 2008). The resulting oligonucleotides, 5′-ctagtTCGCATCTTCGCACGTTACAAtctcgctgatcggcaccatgggggtggt ggtgatcagcgctaTTGTTACGTGCGAAGATGCGAg-3′ and 5′-ctagcTCGCATC TTCGCACGTAACAAtagcgctgatcaccaccaccccatggtgccgatcagcgagaTTGTAAC GTGCGAAGATGCGAa-3′ (uppercase sequences indicate the amiRNA duplex) were annealed by boiling and gradual temperature reduction in a thermocycler and ligated into *SpeI*-digested pChlamiRNA2 (Molnár et al., 2007), yielding pMS668. Correct constructs were screened as described by Molnár et al. (2007). Transformations were carried out with *Chlamydomonas* strain cw15-325 with 1 μg of *HindIII*-linearized pMS668 using the glass beads method (Kindle, 1990).

MS Sample Preparation and Analysis

^{15}N-Labeling of the CC-4533 wild type and *deg1c* mutant line and cell harvests were done as described previously (Mühlhaus et al., 2011). ^{15}N-labeled reference cells were mixed with nonlabeled samples at a $^{15}N/^{14}N$ ratio of 0.8 based on protein content determined by the Lowry assay (Lowry et al., 1951). MS sample preparation was done basically as described (Müller et al., 2018), with minor modifications. In brief, 50 μg of mixed proteins were separated by SDS-PAGE until the proteins had migrated ~1 cm into the separating gel. Proteins were stained with colloidal Coomassie G and the protein-containing gel slice was cut out. Proteins were then digested in gel with trypsin and desalted on home-made STAGE tips (Rappsilber et al., 2007). Peptide analysis via LC-MS/MS (Eksigent nano-LC 425 coupled to TripleTOF 6600; ABSciex) was performed as described (Müller et al., 2018), but using a 66-min gradient for peptide separation. One MS survey scan (350–1,250 *m/z*, 250 ms accumulation time) triggered 20 MS/MS scans (100–1,500 *m/z*, 60 ms accumulation time, rolling collision energy) on the most intense precursors with an intensity >500 centipoise, resulting in a 1.5-s cycle time. After MS/MS analysis, the selected precursors were excluded for 8 s from the analysis.

MS data analysis was carried out using the libraries BioFSharp.Mz (https://github.com/CSBiology/BioFSharp.Mz) and MzLite (https://github.com/CSBiology/MzLite). Peptide identification was based on the computed cross-correlation between theoretical and measured spectra with mass tolerance of 25 ppm and up to three missed cleavages considering ^{14}N light and ^{15}N heavy stable isotopes. The peptide sequences were generated by in silico digestion using version JGI5.5 of the *C. reinhardtii* genome. The calculation of peptide ratios was based on quantification of peak areas of ^{15}N heavy ions and ^{14}N light ions. The efficiency of ^{15}N incorporation in the labeled peptides was estimated according to Schaff et al. (2008). $^{14}N/^{15}N$ ratios were normalized for each peptide by the median of $^{14}N/^{15}N$ ratios of all measured peptides per sample. The mean was calculated from three biological and three technical replicates. The MS proteomics data have been deposited in the ProteomeXchange Consortium via the PRIDE partner repository with the dataset identifier PXD015166.

Electrochromism and Fluorescence Measurements

Fluorescence and absorbance measurements were performed with a Joliot Type Spectrophotometer (Biologic). Absorbance changes due to ECS were measured at 520 nm, and the cytochrome contribution to the signal was removed by subtracting the 547 nm absorbance changes. Fluorescence yields were sampled using 420 nm short detecting pulses. Probing pulses were produced using a broad-band Light Emitting Diode (LED) filtered through interference filters. For ECS and fluorescence measurements, the light-detecting photodiode was protected from actinic light by two specific mechanisms: cutoff filters prevented actinic light from reaching the photodiode (BG39 and BG49 coupled with a high-pass filter for electrochromism and fluorescence measurements, respectively), and actinic light was turned off for 200 μs while the detecting flashes were fired. F_v/F_m was calculated as $(F_m - F_0)/F_m$, with F_0 the fluorescence yield measured in dark-adapted samples and F_m the maximal fluorescence yield measured after a 250-ms saturating actinic pulse of ~2,000 photons m^{-2} s^{-1} (Genty et al., 1989). The light dependency of photosynthesis was fitted by $V_p = V_{max}(1 - \exp(-E/E_k))$ (Platt et al., 1980).

Statistical Analyses

For analysis of the proteomics data, samples were normalized using a method specific for equal protein content to minimize technical influences. For assessing significant changes of proteins, the data were log2 transformed and tested by Student's *t* test assuming unequal variance using a significance threshold (q-value < = 0.1) after correction for multiple hypothesis testing using the q-value method with bootstrapping for $\pi 0$ estimation (Storey, 2002). The analysis was performed using Microsoft F# functional programming language with the bioinformatics library FSharpBio (available on GitHub; https://github.com/CSBiology/BioFSharp). Differential analysis in other pairwise settings was performed with a Student's *t* test assuming equal variance.

Accession Numbers

The accession numbers for *Chlamydomonas* genes *DEG1A*, *DEG1B*, and *DEG1C* are Cre02.g088400, Cre14.g630550, and Cre12.g498500, respectively. The *deg1c* mutant strain from the CLiP library is LMJ.RY0402.139586.

Supplemental Data

The following supplemental materials are available.

Supplemental Figure S1. DEG1C is a Ser protease and proteolytic activity against casein depends on the pH value and the incubation temperature.

Supplemental Figure S2. Peptide coverage of DEG1C and DEG1B proteins immunoprecipitated from *Chlamydomonas* soluble proteins with affinity-purified antibodies against DEG1C.

Supplemental Figure S3. Analysis of DEG1C-depleted lines generated by amiRNA or by insertional mutagenesis.

Supplemental Figure S4. Phenotypical characterization of *DEG1C*-amiRNA mutants under standard growth conditions.

Supplemental Figure S5. Comparison of PSII maximum quantum efficiency, chlorophyll content, and growth between control and *DEG1C*-amiRNA lines exposed to heat stress.

Supplemental Figure S6. Comparison of PSII maximum quantum efficiency between the wild type (black) and *deg1c* mutant (red) under high light and heat.

Supplemental Figure S7. Comparison of photosynthetic electron flow between *deg1c* mutant and wild type.

Supplemental Figure S8. Comparison of ATPase activity, membrane permeability, and ATP/ADP ratio in the dark between *deg1c* mutant and wild type.

Supplemental Figure S9. Alignment of amino acid sequences from Deg1 homologs of selected members of the streptophytes and Chlamydomonadales.

Supplemental Table S1. Results from quantitative shotgun proteomics comparing the *deg1c* mutant with the wild type.

ACKNOWLEDGMENTS

We thank Anja Meffert and Karin Gries for excellent technical help, Hideya Fukuzawa for the antiserum against LCIB, and Frédéric Chaux and Benjamin Bailleul for advice and stimulating discussions.

Received September 1, 2019; accepted September 27, 2019; published October 11, 2019.

LITERATURE CITED

Bailleul B, Cardol P, Breyton C, Finazzi G (2010) Electrochromism: A useful probe to study algal photosynthesis. Photosynth Res **106:** 179–189

Butenko Y, Lin A, Naveh L, Kupervaser M, Levin Y, Reich Z, Adam Z (2018) Differential roles of the thylakoid lumenal Deg protease homologs in chloroplast proteostasis. Plant Physiol **178:** 1065–1080

Caverzan A, Passaia G, Rosa SB, Ribeiro CW, Lazzarotto F, Margis-Pinheiro M (2012) Plant responses to stresses: Role of ascorbate peroxidase in the antioxidant protection. Genet Mol Biol **35**(4 (suppl)): 1011–1019

Chang Z (2016) The function of the DegP (HtrA) protein: Protease versus chaperone. IUBMB Life **68:** 904–907

Chassin Y, Kapri-Pardes E, Sinvany G, Arad T, Adam Z (2002) Expression and characterization of the thylakoid lumen protease DegP1 from Arabidopsis. Plant Physiol **130:** 857–864

Chen X, Kindle KL, Stern DB (1995) The initiation codon determines the efficiency but not the site of translation initiation in *Chlamydomonas* chloroplasts. Plant Cell **7:** 1295–1305

Clausen T, Kaiser M, Huber R, Ehrmann M (2011) HTRA proteases: Regulated proteolysis in protein quality control. Nat Rev Mol Cell Biol **12:** 152–162

Clausen T, Southan C, Ehrmann M (2002) The HtrA family of proteases: Implications for protein composition and cell fate. Mol Cell **10:** 443–455

Eriksson M, Gardestrom P, Samuelsson G (1995) Isolation, purification, and characterization of mitochondria from *Chlamydomonas reinhardtii*. Plant Physiol **107:** 479–483

Fan DY, Nie Q, Hope AB, Hillier W, Pogson BJ, Chow WS (2007) Quantification of cyclic electron flow around Photosystem I in spinach leaves during photosynthetic induction. Photosynth Res **94:** 347–357

Fischer BB, Krieger-Liszkay A, Eggen RIL (2005) Oxidative stress induced by the photosensitizers neutral red (type I) or rose bengal (type II) in the light causes different molecular responses in *Chlamydomonas reinhardtii*. Plant Sci **168:** 747–759

Ge X, Wang R, Ma J, Liu Y, Ezemaduka AN, Chen PR, Fu X, Chang Z (2014) DegP primarily functions as a protease for the biogenesis of β-barrel outer membrane proteins in the Gram-negative bacterium *Escherichia coli*. FEBS J **281:** 1226–1240

Genty B, Briantais JM, Baker NR (1989) The relationship between the quantum yield of photosynthetic electron transport and quenching of chlorophyll fluorescence. Biochim Biophys Acta **990:** 87–92

Girolomoni L, Ferrante P, Berteotti S, Giuliano G, Bassi R, Ballottari M (2017) The function of LHCBM4/6/8 antenna proteins in *Chlamydomonas reinhardtii*. J Exp Bot **68:** 627–641

Göhre V, Ossenbühl F, Crèvecoeur M, Eichacker LA, Rochaix JD (2006) One of two Alb3 proteins is essential for the assembly of the photosystems and for cell survival in *Chlamydomonas*. Plant Cell **18:** 1454–1466

Hammel A, Zimmer D, Sommer F, Mühlhaus T, Schroda M (2018) Absolute quantification of major photosynthetic protein complexes in *Chlamydomonas reinhardtii* using quantification concatamers (QconCATs). Front Plant Sci **9:** 1265

Hansen G, Hilgenfeld R (2013) Architecture and regulation of HtrA-family proteins involved in protein quality control and stress response. Cell Mol Life Sci **70:** 761–775

Hasselblatt H, Kurzbauer R, Wilken C, Krojer T, Sawa J, Kurt J, Kirk R, Hasenbein S, Ehrmann M, Clausen T (2007) Regulation of the σE stress response by DegS: How the PDZ domain keeps the protease inactive in the resting state and allows integration of different OMP-derived stress signals upon folding stress. Genes Dev **21:** 2659–2670

Haussühl K, Andersson B, Adamska I (2001) A chloroplast DegP2 protease performs the primary cleavage of the photodamaged D1 protein in plant photosystem II. EMBO J **20:** 713–722

Höhner R, Barth J, Magneschi L, Jaeger D, Niehues A, Bald T, Grossman A, Fufezan C, Hippler M (2013) The metabolic status drives acclimation of iron deficiency responses in *Chlamydomonas reinhardtii* as revealed by proteomics based hierarchical clustering and reverse genetics. Mol Cell Proteomics **12:** 2774–2790

Itzhaki H, Naveh L, Lindahl M, Cook M, Adam Z (1998) Identification and characterization of DegP, a serine protease associated with the luminal side of the thylakoid membrane. J Biol Chem **273:** 7094–7098

Jiang J, Zhang X, Chen Y, Wu Y, Zhou ZH, Chang Z, Sui SF (2008) Activation of DegP chaperone-protease via formation of large cage-like oligomers upon binding to substrate proteins. Proc Natl Acad Sci USA **105:** 11939–11944

Johnson X (2011) Manipulating RuBisCO accumulation in the green alga, *Chlamydomonas reinhardtii*. Plant Mol Biol **76:** 397–405

Joliot P, Joliot A (2008) Quantification of the electrochemical proton gradient and activation of ATP synthase in leaves. Biochim Biophys Acta **1777:** 676–683

Jomaa A, Iwanczyk J, Tran J, Ortega J (2009) Characterization of the autocleavage process of the *Escherichia coli* HtrA protein: Implications for its physiological role. J Bacteriol **191:** 1924–1932

Jovanovic G, Mehta P, McDonald C, Davidson AC, Uzdavinys P, Ying L, Buck M (2014) The N-terminal amphipathic helices determine regulatory and effector functions of phage shock protein A (PspA) in *Escherichia coli*. J Mol Biol **426:** 1498–1511

Kapri-Pardes E, Naveh L, Adam Z (2007) The thylakoid lumen protease Deg1 is involved in the repair of photosystem II from photoinhibition in *Arabidopsis*. Plant Cell **19:** 1039–1047

Kim KI, Park SC, Kang SH, Cheong GW, Chung CH (1999) Selective degradation of unfolded proteins by the self-compartmentalizing HtrA protease, a periplasmic heat shock protein in *Escherichia coli*. J Mol Biol **294:** 1363–1374

Kindle KL (1990) High-frequency nuclear transformation of *Chlamydomonas reinhardtii*. Proc Natl Acad Sci USA **87:** 1228–1232

Kley J, Schmidt B, Boyanov B, Stolt-Bergner PC, Kirk R, Ehrmann M, Knopf RR, Naveh L, Adam Z, Clausen T (2011) Structural adaptation of the plant protease Deg1 to repair photosystem II during light exposure. Nat Struct Mol Biol **18:** 728–731

Knopf RR, Adam Z (2018) Lumenal exposed regions of the D1 protein of PSII are long enough to be degraded by the chloroplast Deg1 protease. Sci Rep **8:** 5230

Kolmar H, Waller PR, Sauer RT (1996) The DegP and DegQ periplasmic endoproteases of *Escherichia coli*: Specificity for cleavage sites and substrate conformation. J Bacteriol **178:** 5925–5929

Kosuge K, Tokutsu R, Kim E, Akimoto S, Yokono M, Ueno Y, Minagawa J (2018) LHCSR1-dependent fluorescence quenching is mediated by excitation energy transfer from LHCII to photosystem I in *Chlamydomonas reinhardtii*. Proc Natl Acad Sci USA **115:** 3722–3727

Krojer T, Garrido-Franco M, Huber R, Ehrmann M, Clausen T (2002) Crystal structure of DegP (HtrA) reveals a new protease-chaperone machine. Nature **416:** 455–459

Krojer T, Sawa J, Huber R, Clausen T (2010) HtrA proteases have a conserved activation mechanism that can be triggered by distinct molecular cues. Nat Struct Mol Biol **17:** 844–852

Krojer T, Sawa J, Schäfer E, Saibil HR, Ehrmann M, Clausen T (2008) Structural basis for the regulated protease and chaperone function of DegP. Nature **453:** 885–890

Kropat J, Hong-Hermesdorf A, Casero D, Ent P, Castruita M, Pellegrini M, Merchant SS, Malasarn D (2011) A revised mineral nutrient supplement increases biomass and growth rate in *Chlamydomonas reinhardtii*. Plant J **66:** 770–780

Laemmli UK (1970) Cleavage of structural proteins during the assembly of the head of bacteriophage T4. Nature **227:** 680–685

Lemaire C, Wollman FA (1989) The chloroplast ATP synthase in *Chlamydomonas reinhardtii*. I. Characterization of its nine constitutive subunits. J Biol Chem **264:** 10228–10234

Li X, Zhang R, Patena W, Gang SS, Blum SR, Ivanova N, Yue R, Robertson JM, Lefebvre PA, Fitz-Gibbon ST, et al (2016) An indexed, mapped mutant library enables reverse genetics studies of biological processes in *Chlamydomonas reinhardtii*. Plant Cell **28:** 367–387

Lipinska B, Fayet O, Baird L, Georgopoulos C (1989) Identification, characterization, and mapping of the *Escherichia coli htrA* gene, whose product is essential for bacterial growth only at elevated temperatures. J Bacteriol **171:** 1574–1584

Lipinska B, Zylicz M, Georgopoulos C (1990) The HtrA (DegP) protein, essential for *Escherichia coli* survival at high temperatures, is an endopeptidase. J Bacteriol **172:** 1791–1797

Liu C, Willmund F, Whitelegge JP, Hawat S, Knapp B, Lodha M, Schroda M (2005) J-domain protein CDJ2 and HSP70B are a plastidic chaperone pair that interacts with vesicle-inducing protein in plastids 1. Mol Biol Cell **16:** 1165–1177

Lowry OH, Rosebrough NJ, Farr AL, Randall RJ (1951) Protein measurement with the Folin phenol reagent. J Biol Chem **193:** 265–275

Luciński R, Misztal L, Samardakiewicz S, Jackowski G (2011) The thylakoid protease Deg2 is involved in stress-related degradation of the photosystem II light-harvesting protein Lhcb6 in *Arabidopsis thaliana*. New Phytol **192:** 74–86

Malnoë A, Wang F, Girard-Bascou J, Wollman FA, de Vitry C (2014) Thylakoid FtsH protease contributes to photosystem II and cytochrome b_6f remodeling in *Chlamydomonas reinhardtii* under stress conditions. Plant Cell **26:** 373–390

McDonald C, Jovanovic G, Ces O, Buck M (2015) Membrane stored curvature elastic stress modulates recruitment of maintenance proteins PspA and Vipp1. MBio **6:** e01188-15

McDonald C, Jovanovic G, Wallace BA, Ces O, Buck M (2017) Structure and function of PspA and Vipp1 N-terminal peptides: Insights into the membrane stress sensing and mitigation. Biochim Biophys Acta Biomembr **1859:** 28–39

Merdanovic M, Mamant N, Meltzer M, Poepsel S, Auckenthaler A, Melgaard R, Hauske P, Nagel-Steger L, Clarke AR, Kaiser M, et al (2010) Determinants of structural and functional plasticity of a widely conserved protease chaperone complex. Nat Struct Mol Biol **17:** 837–843

Molnár A, Schwach F, Studholme DJ, Thuenemann EC, Baulcombe DC (2007) miRNAs control gene expression in the single-cell alga *Chlamydomonas reinhardtii*. Nature **447:** 1126–1129

Moseley JL, Chang CW, Grossman AR (2006) Genome-based approaches to understanding phosphorus deprivation responses and PSR1 control in *Chlamydomonas reinhardtii*. Eukaryot Cell **5:** 26–44

Mühlhaus T, Weiss J, Hemme D, Sommer F, Schroda M (2011) Quantitative shotgun proteomics using a uniform 15N-labeled standard to monitor proteome dynamics in time course experiments reveals new insights into the heat stress response of Chlamydomonas reinhardtii. Mol Cell Proteomics **10:** M110.004739

Müller N, Leroch M, Schumacher J, Zimmer D, Könnel A, Klug K, Leisen T, Scheuring D, Sommer F, Mühlhaus T, et al (2018) Investigations on VELVET regulatory mutants confirm the role of host tissue acidification and secretion of proteins in the pathogenesis of *Botrytis cinerea*. New Phytol **219:** 1062–1074

Muranaka LS, Rütgers M, Bujaldon S, Heublein A, Geimer S, Wollman FA, Schroda M (2016) TEF30 interacts with photosystem II monomers and is involved in the repair of photodamaged photosystem II in *Chlamydomonas reinhardtii*. Plant Physiol **170:** 821–840

Murwantoko, Yano M, Ueta Y, Murasaki A, Kanda H, Oka C, Kawaichi M (2004) Binding of proteins to the PDZ domain regulates proteolytic activity of HtrA1 serine protease. Biochem J **381:** 895–904

Nordhues A, Schöttler MA, Unger AK, Geimer S, Schönfelder S, Schmollinger S, Rütgers M, Finazzi G, Soppa B, Sommer F, et al (2012) Evidence for a role of VIPP1 in the structural organization of the photosynthetic apparatus in *Chlamydomonas*. Plant Cell **24:** 637–659

Ossowski S, Schwab R, Weigel D (2008) Gene silencing in plants using artificial microRNAs and other small RNAs. Plant J **53:** 674–690

Pallen MJ, Wren BW (1997) The HtrA family of serine proteases. Mol Microbiol **26:** 209–221

Park JJ, Wang H, Gargouri M, Deshpande RR, Skepper JN, Holguin FO, Juergens MT, Shachar-Hill Y, Hicks LM, Gang DR (2015) The response of *Chlamydomonas reinhardtii* to nitrogen deprivation: A systems biology analysis. Plant J **81:** 611–624

Pierre Y, Popot JL (1993) Identification of two 4-kDa miniproteins in the cytochrome b_6f complex from *Chlamydomonas reinhardtii*. C R Acad Sci III **316:** 1404–1409

Plancke C, Vigeolas H, Höhner R, Roberty S, Emonds-Alt B, Larosa V, Willamme R, Duby F, Onga Dhali D, et al (2014) Lack of isocitrate lyase in *Chlamydomonas* leads to changes in carbon metabolism and in the response to oxidative stress under mixotrophic growth. Plant J **77:** 404–417

Platt T, Gallegos CL, Harrison WG (1980) Photoinhibition of photosynthesis in natural assemblages of marine phytoplankton. J Mar Res **38:** 687–701

Ramundo S, Casero D, Mühlhaus T, Hemme D, Sommer F, Crèvecoeur M, Rahire M, Schroda M, Rusch J, Goodenough U, et al (2014) Conditional depletion of the *Chlamydomonas* chloroplast ClpP protease activates nuclear genes involved in autophagy and plastid protein quality control. Plant Cell **26:** 2201–2222

Rappsilber J, Mann M, Ishihama Y (2007) Protocol for micro-purification, enrichment, pre-fractionation and storage of peptides for proteomics using StageTips. Nat Protoc **2:** 1896–1906

Ries F, Carius Y, Rohr M, Gries K, Keller S, Lancaster CRD, Willmund F (2017) Structural and molecular comparison of bacterial and eukaryotic trigger factors. Sci Rep **7:** 10680

Rohr M, Ries F, Herkt C, Gotsmann VL, Westrich LD, Gries K, Trösch R, Christmann J, Chaux-Jukic F, Jung M, et al (2019) The role of plastidic trigger factor serving protein biogenesis in green algae and land plants. Plant Physiol **179:** 1093–1110

Roose JL, Pakrasi HB (2008) The Psb27 protein facilitates manganese cluster assembly in photosystem II. J Biol Chem **283:** 4044–4050

Rütgers M, Muranaka LS, Mühlhaus T, Sommer F, Thoms S, Schurig J, Willmund F, Schulz-Raffelt M, Schroda M (2017a) Substrates of the chloroplast small heat shock proteins 22E/F point to thermolability as a regulative switch for heat acclimation in *Chlamydomonas reinhardtii*. Plant Mol Biol **95:** 579–591

Rütgers M, Muranaka LS, Schulz-Raffelt M, Thoms S, Schurig J, Willmund F, Schroda M (2017b) Not changes in membrane fluidity but proteotoxic stress triggers heat shock protein expression in *Chlamydomonas reinhardtii*. Plant Cell Environ **40:** 2987–3001

Schaff JE, Mbeunkui F, Blackburn K, Bird DM, Goshe MB (2008) SILIP: A novel stable isotope labeling method for in planta quantitative proteomic analysis. Plant J **56:** 840–854

Schägger H, Cramer WA, von Jagow G (1994) Analysis of molecular masses and oligomeric states of protein complexes by blue native electrophoresis and isolation of membrane protein complexes by two-dimensional native electrophoresis. Anal Biochem **217:** 220–230

Schägger H, von Jagow G (1991) Blue native electrophoresis for isolation of membrane protein complexes in enzymatically active form. Anal Biochem **199:** 223–231

Schroda M, Hemme D, Mühlhaus T (2015) The *Chlamydomonas* heat stress response. Plant J **82:** 466–480

Schroda M, Vallon O (2009) Chaperones and Proteases. In DB Stern, ed, The *Chlamydomonas* Sourcebook, Ed 2, Vol **Vol 2**. Elsevier/Academic Press, San Diego, pp 671–730

Schroda M, Vallon O, Whitelegge JP, Beck CF, Wollman FA (2001) The chloroplastic GrpE homolog of *Chlamydomonas*: Two isoforms generated by differential splicing. Plant Cell **13:** 2823–2839

Schroda M, Vallon O, Wollman FA, Beck CF (1999) A chloroplast-targeted heat shock protein 70 (HSP70) contributes to the photoprotection and repair of photosystem II during and after photoinhibition. Plant Cell **11:** 1165–1178

Schuhmann H, Huesgen PF, Adamska I (2012) The family of Deg/HtrA proteases in plants. BMC Plant Biol **12:** 52

Shen QT, Bai XC, Chang LF, Wu Y, Wang HW, Sui SF (2009) Bowl-shaped oligomeric structures on membranes as DegP's new functional forms in protein quality control. Proc Natl Acad Sci USA **106:** 4858–4863

Sinvany-Villalobo G, Davydov O, Ben-Ari G, Zaltsman A, Raskind A, Adam Z (2004) Expression in multigene families. Analysis of chloroplast and mitochondrial proteases. Plant Physiol **135:** 1336–1345

Skórko-Glonek J, Zurawa D, Tanfani F, Scirè A, Wawrzynów A, Narkiewicz J, Bertoli E, Lipińska B (2003) The N-terminal region of HtrA heat shock protease from *Escherichia coli* is essential for stabilization of HtrA primary structure and maintaining of its oligomeric structure. Biochim Biophys Acta **1649:** 171–182

Spiess C, Beil A, Ehrmann M (1999) A temperature-dependent switch from chaperone to protease in a widely conserved heat shock protein. Cell **97:** 339–347

Storey JD (2002) A direct approach to false discovery rates. J R Stat Soc Series B Stat Methodol **64:** 479–498

Strauch KL, Beckwith J (1988) An *Escherichia coli* mutation preventing degradation of abnormal periplasmic proteins. Proc Natl Acad Sci USA **85:** 1576–1580

Ströher E, Dietz KJ (2008) The dynamic thiol-disulphide redox proteome of the *Arabidopsis thaliana* chloroplast as revealed by differential electrophoretic mobility. Physiol Plant **133:** 566–583

Sun X, Fu T, Chen N, Guo J, Ma J, Zou M, Lu C, Zhang L (2010a) The stromal chloroplast Deg7 protease participates in the repair of photosystem II after photoinhibition in Arabidopsis. Plant Physiol **152:** 1263–1273

Sun X, Ouyang M, Guo J, Ma J, Lu C, Adam Z, Zhang L (2010b) The thylakoid protease Deg1 is involved in photosystem-II assembly in *Arabidopsis thaliana*. Plant J **62:** 240–249

Sun X, Peng L, Guo J, Chi W, Ma J, Lu C, Zhang L (2007) Formation of DEG5 and DEG8 complexes and their involvement in the degradation of photodamaged photosystem II reaction center D1 protein in *Arabidopsis*. Plant Cell **19:** 1347–1361

Terashima M, Specht M, Naumann B, Hippler M (2010) Characterizing the anaerobic response of *Chlamydomonas reinhardtii* by quantitative proteomics. Mol Cell Proteomics **9:** 1514–1532

Theis J, Schroda M (2016) Revisiting the photosystem II repair cycle. Plant Signal Behav **11:** e1218587

Truebestein L, Tennstaedt A, Mönig T, Krojer T, Canellas F, Kaiser M, Clausen T, Ehrmann M (2011) Substrate-induced remodeling of the active site regulates human HTRA1 activity. Nat Struct Mol Biol **18:** 386–388

Uniacke J, Colón-Ramos D, Zerges W (2011) FISH and immunofluorescence staining in *Chlamydomonas*. Methods Mol Biol **714:** 15–29

Walter B, Hristou A, Nowaczyk MM, Schünemann D (2015) In vitro reconstitution of co-translational D1 insertion reveals a role of the cpSec-Alb3 translocase and Vipp1 in photosystem II biogenesis. Biochem J **468:** 315–324

Walters RG, Shephard F, Rogers JJ, Rolfe SA, Horton P (2003) Identification of mutants of Arabidopsis defective in acclimation of photosynthesis to the light environment. Plant Physiol **131:** 472–481

Weiss D, Schneider G, Niemann B, Guttmann P, Rudolph D, Schmahl G (2000) Computed tomography of cryogenic biological specimens based on X-ray microscopic images. Ultramicroscopy **84:** 185–197

Willmund F, Dorn KV, Schulz-Raffelt M, Schroda M (2008) The chloroplast DnaJ homolog CDJ1 of *Chlamydomonas reinhardtii* is part of a multichaperone complex containing HSP70B, CGE1, and HSP90C. Plant Physiol **148:** 2070–2082

Willmund F, Schroda M (2005) HEAT SHOCK PROTEIN 90C is a bona fide Hsp90 that interacts with plastidic HSP70B in *Chlamydomonas reinhardtii*. Plant Physiol **138:** 2310–2322

Wingler A, Lea PJ, Quick WP, Leegood RC (2000) Photorespiration: Metabolic pathways and their role in stress protection. Philos Trans R Soc Lond B Biol Sci **355:** 1517–1529

Witt HT (1979) Energy conversion in the functional membrane of photosynthesis. Analysis by light pulse and electric pulse methods. The central role of the electric field. Biochim Biophys Acta **505:** 355–427

Wong-Ekkabut J, Xu Z, Triampo W, Tang IM, Tieleman DP, Monticelli L (2007) Effect of lipid peroxidation on the properties of lipid bilayers: A molecular dynamics study. Biophys J **93:** 4225–4236

Yamano T, Miura K, Fukuzawa H (2008) Expression analysis of genes associated with the induction of the carbon-concentrating mechanism in *Chlamydomonas reinhardtii*. Plant Physiol **147:** 340–354

Zerges W, Rochaix JD (1998) Low density membranes are associated with RNA-binding proteins and thylakoids in the chloroplast of *Chlamydomonas reinhardtii*. J Cell Biol **140:** 101–110

Zhang L, Kato Y, Otters S, Vothknecht UC, Sakamoto W (2012) Essential role of VIPP1 in chloroplast envelope maintenance in *Arabidopsis*. Plant Cell **24:** 3695–3707

Zhang L, Kusaba M, Tanaka A, Sakamoto W (2016) Protection of chloroplast membranes by VIPP1 rescues aberrant seedling development in *Arabidopsis nyc1* mutant. Front Plant Sci **7:** 533

Zhang Z, Shrager J, Jain M, Chang CW, Vallon O, Grossman AR (2004) Insights into the survival of *Chlamydomonas reinhardtii* during sulfur starvation based on microarray analysis of gene expression. Eukaryot Cell **3:** 1331–1348

Zienkiewicz M, Ferenc A, Wasilewska W, Romanowska E (2012) High light stimulates Deg1-dependent cleavage of the minor LHCII antenna proteins CP26 and CP29 and the PsbS protein in *Arabidopsis thaliana*. Planta **235:** 279–288